Metric and morphological study of the upper cervical spine from the Sima de los Huesos site (Sierra de Atapuerca, Burgos, Spain)

Asier Gómez-Olivencia [a,b,*], José Miguel Carretero [a,b], Juan Luis Arsuaga [b,c], Laura Rodríguez-García [a,b], Rebeca García-González [a,b], Ignacio Martínez [b,d]

[a] *Laboratorio de Evolución Humana. Dpto. de Ciencias Históricas y Geografía. Universidad de Burgos. Edificio I+D+i. Plaza Misael de Bañuelos s/n. 09001 Burgos, Spain*

[b] *Centro UCM-ISCIII de Investigación sobre Evolución y Comportamiento Humanos, c/Sinesio Delgado, 4 (Pabellón 14), 28029 Madrid, Spain*

[c] *Departamento de Paleontología, Facultad de Ciencias Geológicas, Universidad Complutense de Madrid, Ciudad Universitaria s/n, 28040 Madrid, Spain*

[d] *Departamento de Geología, Universidad de Alcalá, Edificio de Ciencias, Campus Universitario, 28871 Alcalá de Henares, Spain*

Abstract

In this article, the upper cervical spine remains recovered from the Sima de los Huesos (SH) middle Pleistocene site in the Sierra de Atapuerca (Burgos, Spain) are described and analyzed. To date, this site has yielded more than 5000 human fossils belonging to a minimum of 28 individuals of the species *Homo heidelbergensis*. At least eleven individuals are represented by the upper cervical (C1 and C2) specimens: six adults and five subadults, one of which could represent an adolescent individual. The most complete adult vertebrae (three atlases and three axes) are described, measured, and compared with other fossil hominins and modern humans. These six specimens are associated with one another and represent three individuals. In addition, one of these sets of cervical vertebrae is associated with Cranium 5 (Individual XXI) from the site. The metric analysis demonstrates that the Sima de los Huesos atlases and axes are metrically more similar to Neandertals than to our modern human comparative sample. The SH atlases share with Neandertals a sagittally elongated canal. The most remarkable feature of the SH (and Neandertal) axes is that they are craniocaudally low and mediolaterally wide compared to our modern male sample. Morphologically, the SH sample shares with Neandertals a higher frequency of caudally projected anterior atlas arch, which could reflect greater development of the longus colli muscle. In other features, such as the frequency of weakly developed tubercles for the attachment of the transverse ligament of the atlas, the Sima de los Huesos fossils show intermediate frequencies between our modern comparative samples and the Neandertals, which could represent the primitive condition. Our results are consistent with the previous phylogenetic interpretation of *H. heidelbergensis* as an exclusively European species, ancestral only to *H. neanderthalensis*.

Keywords: Atlas; Axis; Cervical vertebrae; Middle Pleistocene; Sima de los Huesos

Introduction

The Sima de los Huesos (SH) site is approximately 0.5 km from the Cueva Mayor entrance, well inside the Cueva Mayor–Cueva del Silo cave system in the Sierra de Atapuerca in northern Spain (Arsuaga et al., 1997b). To date, more than 5000 fossil human remains have been recovered from the site (Arsuaga and Martínez, 2004) in the excavations directed by one of us (JLA). Based on dental evidence, these remains belong to a minimum number of 28 individuals (Bermúdez de Castro et al., 2004) of both sexes and diverse ages. In addition, thousands of carnivore bones have been recovered mixed with and stratigraphically above the human fossils (García et al., 1997; García, 2002). All anatomical parts of the skeleton are represented among the human remains, suggesting that

complete corpses were accumulated at this site. The age-at-death distribution suggests that a nonattritional demographic event affected this living population (Bocquet-Appel and Arsuaga, 1999; Bermúdez de Castro et al., 2004). The origin of the human accumulation is most likely to be anthropogenic (Arsuaga et al., 1997b). A recently discovered handaxe has been interpreted as evidence of symbolic behavior in these early humans (Carbonell et al., 2003).

A recently found in situ speleothem (SRA-3), which seals the human-fossil-bearing sediments throughout the site, has been dated. There is a hiatus in the speleothem growth at about 4 cm below the top. This upper portion shows a linear growth rate of about 1 cm per 32,000 years. Ten dates have been obtained in the lower 10 cm of speleothem below the hiatus, all of which indicate a minimum age of 350 ka, although this thickness could represent a significant amount of time beyond this date. Thus, a range of 400–500 ka has been proposed for the human remains (Bischoff et al., 2003). These dates are compatible with both the micro- and macromammalian assemblages (Cuenca-Bescós et al., 1997; García et al., 1997; García, 2002). Bischoff et al. (2006) recently published a reanalysis of six samples of SRA-3 using inductively coupled plasma-multicollector mass-spectrometry (ICP-MS), which yielded new dates that cluster around 600 ka, with an estimated minimum age of the speleothem, and thus of the underlying human fossils, of 530 ka.

The human remains from this site have been assigned to *Homo heidelbergensis*. This species, in our view, is exclusively European, and is ancestral only to the later Neandertals (Arsuaga et al., 1991, 1997c; Carretero et al., 1997; Martínez and Arsuaga, 1997).

The record of the upper cervical vertebral column is relatively abundant for *Homo neanderthalensis* and late Pleistocene *Homo sapiens*, but with respect to the rest of the genus *Homo*, it is scarce or nonexistent.[1] The virtual absence of a fossil record of the upper cervical spine for the middle Pleistocene underscores the importance of the SH specimens described and analyzed here.

Regarding the Neandertals, the most conspicuous traits described for the atlas vertebra (C1) are (1) weakly developed tubercles for the insertion of the transverse ligament and (2) a caudal projection of the anterior tubercle (Boule, 1911–1913; Martin, 1923; Heim, 1976; Arensburg, 1991); for the Neandertal axis (C2) no trait or pattern has been highlighted except its great morphological variability (Piveteau, 1966). In his study of the cervical spine of the Kebara 2 Neandertal individual, Arensburg (1991) concluded that, except for the horizontal spinous process of the C6 and C7, the cervical column seemed to be within the range of variation of modern human populations. Nevertheless, the study of the middle Pleistocene SH upper cervical vertebrae (C1 and C2) may reveal some previously undocumented morphological features and/or patterns of variation within the Neandertal evolutionary lineage.

The first part of the study comprises the inventory of all the atlases and axes, with the determination (if possible) of the age at death (Tables 3 and 4) and the minimum number of individuals represented among the remains. A brief description of the most complete adult vertebrae is also provided. In the second part, we perform a metrical analysis of the adult vertebrae and compare the anatomical features present in the SH specimens with those found in other samples of *Homo*, especially *H. neanderthalensis* and *H. sapiens*.

Materials

The SH vertebral sample comprises 455 fossils that represent at least 180 vertebrae. The cervical sample consists of 116 fossils (Gómez-Olivencia, 2005), including 22 first cervical vertebrae (atlas) and 16 second cervical vertebrae (axis). The present study includes the atlas (C1) and axis (C2) remains recovered up through the 2004 field season. An inventory and photographic documentation of all the fossil material, as well as short descriptions and metrical data of the most complete adult vertebrae, are provided.

Descriptions of a few of the cervical vertebrae [including the atlas VC3 (AT-1554) and a general description of the SH cervical vertebrae] have been published previously (Carretero et al., 1999; Gómez et al., 2005). The present study provides a detailed analysis of the SH upper cervical spine. Appendix 1 provides information on the labeling of the SH vertebrae.

For comparative purposes we have studied a large sample of modern human skeletons and fossil hominin specimens from the following species: *H. antecessor*, *H. neanderthalensis*, and late Pleistocene *H. sapiens* (Table 1). Although remains of the atlas and axis are also known from the Mousterian site of Qafzeh (Vandermeersch, 1981), their fragmentary nature makes comparison with these specimens difficult. Data for the following specimens have been taken from the literature: Kebara 2 (Arensburg et al., 1990; Arensburg, 1991), Régourdou 1 (Piveteau, 1966), Shanidar 2 and 4 (Stewart, 1962; Trinkaus, 1983), Subalyuk (Pap et al., 1996), and Dolní Věstonice 14 (Sládek et al., 2000).

Methods

We used standard anthropometric techniques and instruments to take all measurements. The metric variables are illustrated in Fig. 1. Following Meyer (2005), the areas of vertebral canals were measured on scaled digital images and cross-checked for accuracy by comparing imaged linear measurements to physical dimensions measured with digital calipers. This method avoids the considerable error of area estimation by simply multiplying the dorsoventral and transverse diameters of the neural canal (Meyer, 2005). Vertebral-canal areas were measured on cranial (atlas) and caudal (axis) photographs using CAD software and cross-checked using the canal's maximum transverse diameter (M11). For the atlas, the photograph was taken in superior view.

[1] The exceptions are the specimens from Dmanisi (Meyer, 2005), Gran Dolina (Carretero et al., 1999), and Koobi Fora (KNM-ER 1808; Walker et al., 1982; Leakey and Walker, 1985) for the early Pleistocene and, for the middle Pleistocene, the atlas from the Zhoukoudian I1 individual (Boaz et al., 2004).

Table 1
Comparative specimens and samples of atlases and axes measured by the authors

Specimen/sample	Species	Sex	Original/cast	Location
ATD6-90 (C1)	*H. antecessor*	Female	Original	Museo de Burgos, Burgos (Spain)
Krapina (C1, $n = 3$; C2, $n = 3$)	*H. neanderthalensis*	?	Original	Croatian Natural History Museum, Zagreb (Croatia)
La Chapelle-aux-Saints (C1 and C2)	*H. neanderthalensis*	Male	Original	Musée de l'Homme, Paris (France)
La Ferrassie 1 (C1 and C2)	*H. neanderthalensis*	Male	Original	Musée de l'Homme, Paris (France)
Shanidar 2 (C1 and C2)	*H. neanderthalensis*	Male	Cast	Musée de l'Homme, Paris (France)
Skhul V (C1 and C2)	*H. sapiens*	Male	Original	Peabody Museum of Archaeology and Ethmology, Cambridge (MA, USA)
Arcy-sur-Cure, Grotte des Fées (C1 and C2)	*H. sapiens* (?)[1]	?	Original (C1) Cast (C2)	Musée de l'Homme, Paris (France) (C1) Institut de Paléontologie Humaine, Paris (France) (C2)
Cro-Magnon (C1)	*H. sapiens*	Male	Original	Musée de l'Homme, Paris (France)
Carolingian[2] (C2, $n = 4$)	*H. sapiens*	?	Original	Musée de l'Homme, Paris (France)
Neolithic[3] (C2, $n = 2$)	*H. sapiens*	?	Original	Musée de l'Homme, Paris (France)
Afalou-Bou-Rhummel[4] (C1, $n = 12$; C2, $n = 10$)	*H. sapiens*	?	Original	Institut de Paléontologie Humaine, Paris (France)
Taforalt[5] (C1, $n = 8$; C2, $n = 9$)	*H. sapiens*	?	Original	Institut de Paléontologie Humaine, Paris (France)
Burgos[6] ($n = 40$)	*H. sapiens*	Males	Original	Laboratorio de Evolución Humana-University of Burgos, Burgos (Spain)
Hamman-Todd[7] ($n = 101$)	*H. sapiens*	50 males/51 females	Original	Cleveland Museum of Natural History, Cleveland (OH, USA)

[1] The Arcy-sur-Cure atlas was found in 1860 in the lower level of the Grotte des Fées, (Yonne, France). The axis was found in 1898 in the clearings of older excavations (Leroi-Gourhan, 1958). Leroi-Gourhan (1958) identified both specimens as Neandertal. In the case of the axis, the taxonomic assignment was based on the surface color of the fossil; Leroi-Gourhan pointed out that this specimen is within the modern human range of variation but that it resembles Neandertals in its weak cervical curvature. In the case of the atlas, he did not find any trait to distinguish it from modern humans. Due to the problematic provenience of both specimens and the fact that these fossils are morphologically more similar to our modern human comparative samples than to Neandertals, they should be cautiously considered as representing *H. sapiens*.

[2] The Carolingian sample comes from the Saint-Germain-des-Prés cemetery (Paris, France).

[3] The Neolithic sample comes from a cave site in the Petit Morin Valley (France).

[4] The Afalou-Bou-Rhummel sample was recovered from the homonymous rock-shelter in Algeria. This sample and the Taforalt sample are dated to >10,000 BP (see Irish, 2000, and references therein).

[5] The Taforalt sample was recovered from the homonymous cave site in Morocco.

[6] The Burgos sample comprises 40 contemporary adult (estimated age at death is 20–45 years) male individuals from Burgos, Spain.

[7] The Hamann-Todd sample comprises 100 North American adults (50 Euro-Americans and 50 Afro-Americans, with equal sexual representation) from the Hamann-Todd Osteological Collection.

Univariate comparative analysis was performed on all of the variables measured in the atlases and axes. Bivariate analysis was performed on the vertebral-canal variables (M10 and M11) in both C1 and C2, and the M1a and STrD measurements in the axes. We used nonparametric methods in cases where one or more of the groups had a sample size of $n < 10$. For the univariate analysis, we performed a Kruskal–Wallis test to compare the differences between the SH, Neandertal, and Burgos modern human samples. When a significant difference ($p < 0.05$) was found in a variable, we performed a Mann–Whitney test between all possible pairs of samples to determine which ones were significantly different. We adjusted the p-values for these comparisons using the Bonferroni method and have reported all the cases in which $p < 0.10$.

Inventory

Here we provide an inventory of all the atlas and axis remains. These fossils are listed in Tables 2 and 3 and depicted in Figs. 2–5. The SH upper cervical sample comprises 22 atlas specimens and 16 axis specimens.

Age at death

The age at death has been estimated for the SH cervical vertebrae (Tables 2 and 3) based on modern human patterns of maturation (i.e., fusion of the principal centers of ossification, presence/absence of the epiphyseal rings, and degree of obliteration of the metaphyseal scars). However, since the SH hominins had a shorter period of dental growth (Ramírez Rozzi and Bermúdez de Castro, 2004), the ages at death might be overestimated if tooth formation is correlated with somatic development, as proposed by Smith (1991).

Given the difficulty of assigning a precise age at death based on the ossification patterns of the atlas (except in limited circumstances), these specimens are classified as adult or subadult. The atlas's principal centers of ossification are fused by the sixth year of life (Scheuer and Black, 2000). Additional attention was given to the surface of the articular facets for the determination of the age at death, since immature individuals show a more porous surface. In the Atapuerca sample, the VC3 atlas shows a partially obliterated metaphyseal scar on its transverse processes. This feature is consistent with the

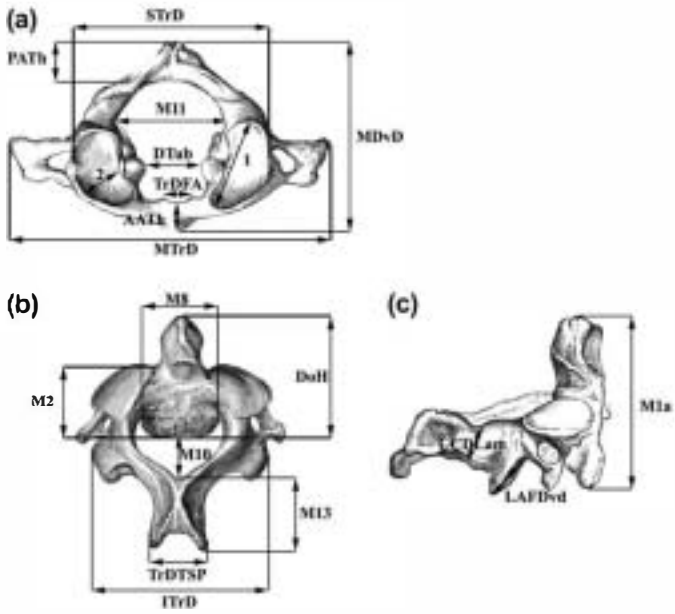

Fig. 1. Some of the dimensions used in the osteometric analysis, as defined in the text: (a) atlas (C1) in cranial view; (b) axis (C2) in craniodorsal view; (c) axis (C2) in lateral view. Drawings modified from Gray (1959). (1) Diameters in major axis of upper articular facets (UAFMAD) (right-left); (2) diameter at a right angle to the major axis of upper articular facets (UAFTrD) (right-left); anterior arch thickness at the level of the anterior tubercle (AATh); craniocaudal diameter of laminae (CCDLam) (right-left); total vertebral dorsal height (DoH); distance between the tubercles for the attachment of the transverse ligament (DTub); inferior transverse diameter (ITrD); lower articular facet dorsoventral diameter (LAFDvD) (right-left); total vertebral ventral height (M1a); body craniocaudal dorsal diameter (M2); body inferior transverse diameter (M8); canal dorsoventral maximum diameter (M10); canal transverse maximum diameter (M11); spine length (M13); maximum dorsoventral diameter (MDvD); maximum transverse diameter (MTrD); posterior arch thickness at the level of the posterior tubercle (PATh); superior transverse diameter (STrD); transverse diameter of the facet for the axis (TrDFA); maximum transverse diameter of the tip of the spinous process (TrDTSP). The following variables have not been drawn: body inferior anteroposterior diameter (M5), taken perpendicular to M8; upper articular facet dorsoventral diameter of the axis (UAFDvD) (right-left); upper articular facet transverse diameter of the axis (UAFTrD) (right-left); lower articular facet transverse diameter (LAFTrD) (right-left), taken perpendicular to LAFDvD; thickness of the laminae (ThLam), taken perpendicular to CCDLam; anterior arch height at the level of the anterior tubercle (AAH), taken perpendicular to AATh; maximum height of lateral masses (right-left) (MHLM), taken at the lateral edges of the lateral masses of the atlas; posterior arch height at the level of the posterior tubercle (PAH), taken perpendicular to PATh; height of the posterior arch in the groove for the vertebral artery (HPAG) (right-left). M# refers to the Martin number (Bräuer, 1988) and variable definition. In the axes, M10 has been measured on the caudal aspect of the vertebral foramen.

age at death estimated (21–25 years) for the associated vertebra VC4(C2). The left mass AT-2078 exhibits the immature appearance on the surface of both articular facets, while VC17 only exhibits this appearance in the upper articular facet.

In contrast to the atlas, the complex ossification pattern of the axis allows for more precise age-at-death estimates. The axis ossifies from five primary centers: one for the body, one for each half of the dens, and one for each half of the neural arch. The halves that form the dens are already fused at birth, whereas the neural arch is fused by the third or fourth year and the body is joined to the other elements by the fifth or sixth year of life. The axis has five secondary centers of ossification: two for the transverse processes; the *ossiculum terminale*, which fuses at the end of the dens by the twelfth year; one for the spine; and an inferior epiphyseal ring, which fuses to the caudal part of the body (Scheuer and Black, 2000). Buikstra et al. (1984) reported that the fusion of the inferior epiphyseal ring commences by 17–19 years and is completed by the twenty-fifth year in their female sample from the Terry Collection. Both VC4 and VC28 show a partial fusion of the caudal epiphyseal ring. Nevertheless, VC4 shows a more advanced state of fusion, so it could belong to an individual who was older than VC28.

Minimum number of individuals

A minimum of 28 individuals, based on the dental remains, have been identified among the SH human fossils (Bermúdez de Castro et al., 2004). Regarding the atlas, a minimum of 10 individuals are represented, based on the repetition of the left mass. In addition, AT-3985 (a right lateral mass) represents another individual due to its incompatibility with any of the left lateral masses. These 11 individuals represent six adults (one of them less than 25 years of age, represented by VC3) and five subadults, one of them possibly an adolescent, represented by VC17 (Table 2). Among the axes, based on the repetition of the most common element (the dens of the axis), at least 10 individuals are recognizable: four adults (one of them less than 25 years of age), one late adolescent or young adult, one immature individual between 12 and 16 years of age, and four individuals older than 12 years. All these ages at death are fully compatible with those based on dental (Bermúdez de Castro et al., 2004), cranial (Arsuaga et al., 1997c), and postcranial evidence (Carretero et al., 1997).

Sex determination

Sex determination of the three most complete SH atlases and axes, which represent three individuals, was attempted based on multiple regression equations and discriminant functions (Marino, 1995; Wescott, 2000). The results suggest that these three sets of upper cervical vertebrae all represent male individuals.

Additionally, a discriminant function was generated from data taken from atlas specimens in the Hamann-Todd Osteological Collection, and we calculated the a posteriori probability of the most complete SH atlases (VC3 and VC7) being classified as belonging to male individuals (Table 4). These two SH atlases show a posteriori probabilities of being from male individuals higher than 0.80. Due to the incompleteness of VC16, it was not possible to apply the discriminant function, but using an additional discriminant function in which only ITrD is used, VC16 is classified as being from a male with an a posteriori probability of 0.79.

Marino's (1995), Wescott's (2000), and our formulae were used to estimate the sex of several additional fossil atlases and axes. The results agree with the sex determinations based on other postcranial features with one exception: the Régourdou 1 individual is classified as being from a male using the

Table 2
Inventory of the atlas (C1) remains from the SH site (as of the 2004 field season)

Specimen number	Year	Preservation	Age at death	Figure
VC3[1]	1995	Complete vertebra	Adult	2a,b,c
VC7[2]	2000	Complete vertebra	Adult	2d,e,f
VC16[3]	1994, 1997	Masses and posterior arch	Adult	2g,h
VC17[4]	1995, 2000	Anterior arch and left mass	Adolescent (?)	3a
AT-269	1989	Left mass	Subadult	3b
AT-326	1990	Left mass		3c
AT-1818	1996	Left mass	Adult	3d
AT-2078	1997	Left mass	Subadult	3e
AT-2130	1997	Anterior arch		3l
AT-2264	1997	Posterior arch	>5 years	3p
AT-2584	1998	Left mass, posterior arch		3f
AT-2852	1998	Anterior arch		3m
AT-3003	1999	Left mass		3g
AT-3013	1999	Right mass, posterior arch fragment	Adult	3h
AT-3687	2000	Posterior arch	Subadult (?)	3q
AT-3691	2000	Posterior arch	Subadult (?)	3r
AT-3693	2000	Anterior arch		3n
AT-3694	2000	Right mass	Subadult	3i
AT-3971	1994	Right mass	Subadult	3j
AT-3985	?	Right mass	Adult	3k
AT-3992	1992	Posterior arch		3s
AT-4037	2000	Anterior arch fragment		3o

[1] VC3 = AT-1554.
[2] VC7 = AT-3339 + AT-3340 + AT-3341 + AT-3688.
[3] VC16 = AT-1140 + AT-2201.
[4] VC17 = AT-3374 + AT-3973 + AT-3991.

Table 3
Inventory of the axis (C2) remains from the SH site (as of the 2004 field season)

Specimen number	Year	Preservation	Age at death	Figure
VC2[1]	1998	Complete vertebra	>25	4a,b,c
VC4[2]	1995	Complete vertebra	17–25 (21–25)?	4d,e,f
VC8[3]	2000, 2001	Complete vertebra	>25	4g,h,i
VC28[4]	2003	Complete except right transverse process	17–25 (17–20)?	5a
AT-150	1988	Right lamina, spinous process	>25	5d
AT-1573	1995	Dens, body, right art. facet, frag. upper left art. facet	12–16	5b
AT-2289	1997	Dens, frag. body, frag. upper right facet	12–16	5c
AT-2883	1998	Dens	>12	5f
AT-3696	2000	Dens	>12	5g
AT-3741	2000	Left superior art. facet	>6	5k
AT-3979	1998	Dens	>12	5h
AT-4046	1994	Frag. laminae, spinous process	4-25	5j
AT-4051	1998	Frag. right lamina, right lower art. facet	>4	5l
AT-4187	2003	Frag. body, right upper art. facet	6–16	5m
AT-4314	2003	Dens	>12	5i
AT-4662	1995	Tip of the spinous process	<25 (16–25)?	5e

[1] VC2 = AT-2465.
[2] VC4 = AT-1555.
[3] VC8 = AT-3680 + AT-3840.
[4] VC28 = AT-4634 + AT-4643.

axis, while its sex has been regarded as indeterminate by Vandermeersch and Trinkaus (1995). On the other hand, Krapina 98 and 104, of unknown sex, were classified as belonging to females. The classification of the Gran Dolina ATD6-90 still agrees with the previous sex determination by Carretero et al. (1999), but the result should be interpreted more cautiously due to its low a posteriori probability (0.67).

The results of the sex determination of the VC7 atlas and VC8 axis are also congruent with the sex assignment of Cranium 5 based on the associated mandible AT-888 (Rosas et al., 2002; Bermúdez de Castro et al., 2004). Although Cranium 5 appears to be a small male or a female when the cranial measurements are compared with other middle Pleistocene fossils and Neandertals, the facial skeleton is large and thus likely that of a male (Arsuaga et al., 1997c).

Brief description of the most complete atlases and axes

Atlases

The most complete adult atlases are shown in Fig. 2.

Specimen VC3(C1) is the most complete nonmodern atlas of a fossil hominin yet found. It preserves the transverse processes, which show an incompletely obliterated metaphyseal line. This vertebra was found in anatomical connection with the VC4 axis. The anterior bar of the left transverse process is not fused to the posterior bar, and this specimen exhibits subtle tubercles for the attachment of the transverse ligament. The transverse processes show a triangular cross section, making the dorsal surface quite vertical.

Specimen VC7(C1) is slightly larger and more robust than VC3. It lacks the transverse processes. The sulcus for the right vertebral artery is covered by a bony arch, while that on the left side is only partially covered. Such foramina are not unusual and have been reported in the atlas of the Shanidar 2 Neandertal (Stewart, 1962; Trinkaus, 1983). Like VC3, this specimen exhibits subtle tubercles for the attachment of the transverse ligament.

Specimen VC16(C1) lacks the anterior arch and the transverse processes. It exhibits severe postmortem erosion to the superior articular facets and inferior left articular facet. It is smaller than the VC3 and VC7 atlases, although the size of its posterior arch falls between that of VC3 and VC7. It also

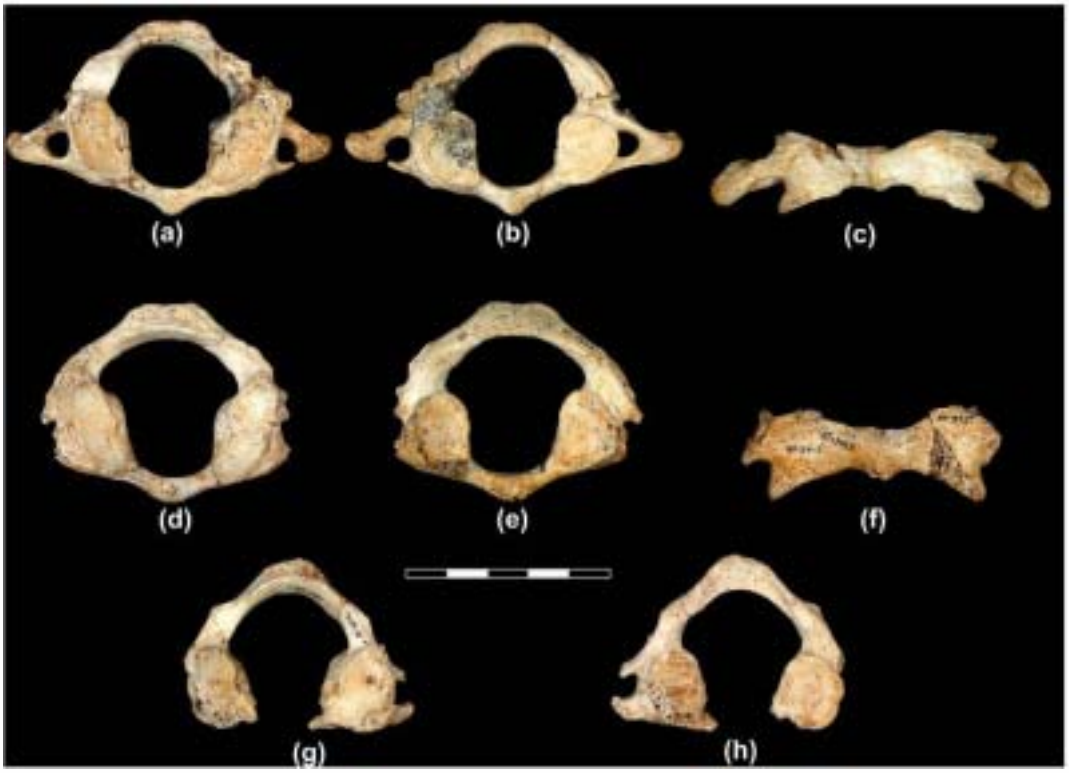

Fig. 2. Complete or nearly complete atlases from Sima de los Huesos. VC3 atlas in cranial (a), caudal (b), and ventral (c) views. VC7 atlas in cranial (d), caudal (e), and ventral (f) views. VC16 atlas in cranial (g), caudal (h), and ventral views. Scale bar = 5 cm.

exhibits more strongly developed tubercles for the attachment of the transverse ligament.

All of the SH atlases possess straight medial edges of the inferior articular facets, a feature that is also found in the Neandertal specimens from La Chapelle-aux-Saints and La Ferrassie 1, while most atlases in our modern human comparative sample from Burgos possess rounded edges. We cannot evaluate this trait in other fossil hominins because this anatomical region suffers erosion [e.g., the Gran Dolina ATD6-90 and KNM-ER 1808 atlases (see Leakey and Walker, 1985)].

Axes

The most complete adult axes are shown in Fig. 4.

Specimen VC2(C2) is a nearly complete axis that lacks only the transverse processes and is eroded at the dorsoinferior (posteroinferior) part of the vertebral body, at both lateral ends of the superior articular surfaces, and at the spinous process. It is attributed to a fully adult individual, as the inferior epiphyseal ring is completely fused. Its size is intermediate between the large axes (VC4 and VC8) and the small axis VC28.

Specimen VC4(C2) is a complete axis that is only slightly eroded on the dorsoinferior (posteroinferior) part of the body, at the tip of the spine, and at the lateral ends of the transverse processes and inferior articular facets. The secondary center of ossification of the spinous process is still unfused, and the inferior epiphyseal ring is in a more advanced state of fusion than VC28. This specimen was found in anatomical connection in the excavation with the VC3 atlas.

Specimen VC8(C2) lacks the transverse processes and bone chips from the vertebral body at the base of the dens, from the tip of the spinous process, and from the ventralmost part of the right superior articular facet. It is slightly worn at the dorsoinferior (posteroinferior) part of the body. It is similar in size to VC4, albeit slightly more robust. The spinous process is clearly bifid.

All of the spinous processes of the SH axes are robust. The axis specimens in the modern human samples that we have studied (Burgos and Hamann-Todd) possess spinous processes with a triangular shape in dorsal view and crowned with a narrow ridge at the cranial end. On the other hand, all the spinous processes of the SH axes possess more vertically oriented lateral walls, and therefore the whole spinous process has a "trapezoidal" and massive appearance. Neandertals that preserve this region show the same pattern [e.g., La Ferrassie 1 (Gómez-Olivencia, personal observation) and Krapina 104 (see Figure 177 in Radovcic et al., 1988: 72)], as do some late Pleistocene modern humans [e.g., Taforalt [redacted] (Gómez-Olivencia, personal observation) and Dolní Věstonice 15 (see Figure 14.4 in Holliday, 2006: 244)]. This pattern could be related to strong development of the nuchal muscles *M. rectus capitis posterior major* and *M. obliquus capitis inferior*.

Associations of vertebrae

Among the atlas and axis remains from the SH site, it has been possible to recognize three associated sets of vertebrae

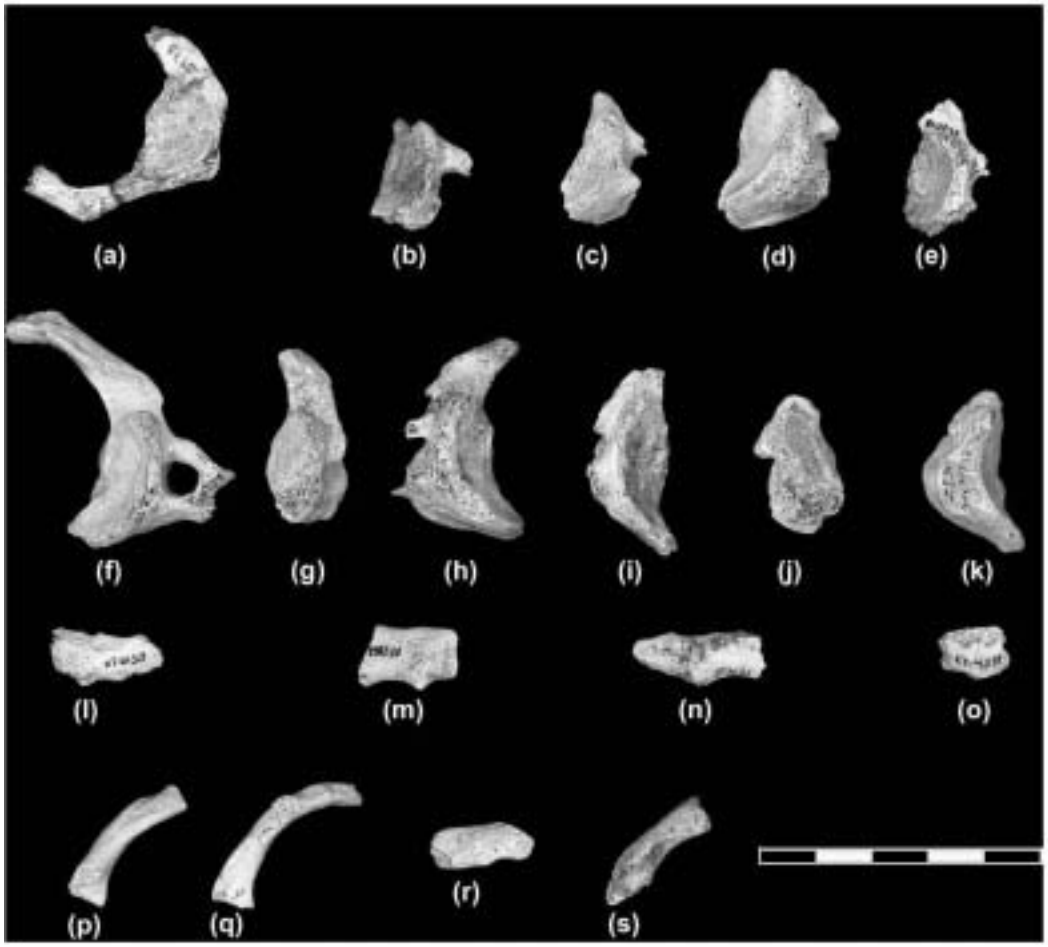

Fig. 3. Sima de los Huesos fragmentary atlases. Cranial view of (a) VC17, (b) AT-269, (c) AT-326, (d) AT-1818, (e) AT-2078, (f) AT-2584, (g) AT-3003, (h) AT-3013, (i) AT-3694, (j) AT-3971, (k) AT-3985. Dorsal view of (l) AT-2130, (m) AT-2852, (n) AT-3693, (o) AT-4037. Cranial view of (p) AT-2264, (q) AT-3687, (r) AT-3691, (s) AT-3992. Scale bar = 5 cm.

based on age at death, size, and anatomical compatibility (articular congruence). These sets are listed below:

- VC3(C1) and VC4(C2): These specimens are the first two cervical vertebrae of a young adult individual of about 21–25 years of age at death based on the degree of fusion of the epiphyses. The atlas was found articulated with the axis.
- VC7(C1) and VC8(C2): These vertebrae belong to an adult individual older than 25 years of age at death based on the complete fusion of the inferior epiphyseal ring. In addition, VC7 (and hence VC8) has been associated with Cranium 5 (Individual XXI; see Bermúdez de Castro et al., 2004) based on size, articular congruence and similar degree of osteophytosis (see below). This association is the first between cranial and postcranial remains from this site.
- VC16(C1) and VC2(C2): These vertebrae belong to an adult individual of more than 25 years of age at death based on the complete fusion of the inferior epiphyseal ring. They exhibit a comparable degree of ossification of the insertion of the articular capsules between C1 and C2.

Morphology and metrics of the atlas

Metrics

The metric dimensions and indices of the SH atlases and comparative data from Neandertal and modern human samples are provided in Tables 5–7. Results of the Kruskal–Wallis test and Mann–Whitney *U*-test are presented in Table 5.

The SH atlases are metrically closer to Neandertals than to our modern human comparative samples; they show a sagittally elongated canal, sagittally expanded inferior articular facets, and a broader inferior transverse diameter. In Neandertals, the sagittal elongation of the atlas is more extreme than in the SH vertebrae. The significantly broader inferior transverse diameter of the SH atlases (ITrD) (compared with both modern human samples) has its counterpart in the significantly broader superior transverse diameter (STrD) of the SH axes (see below).

All the SH indices are well within the ranges of variation of our modern human comparative samples (Table 7). In contrast, Neandertals show a high shape index due to their significantly larger maximum dorsoventral diameter.

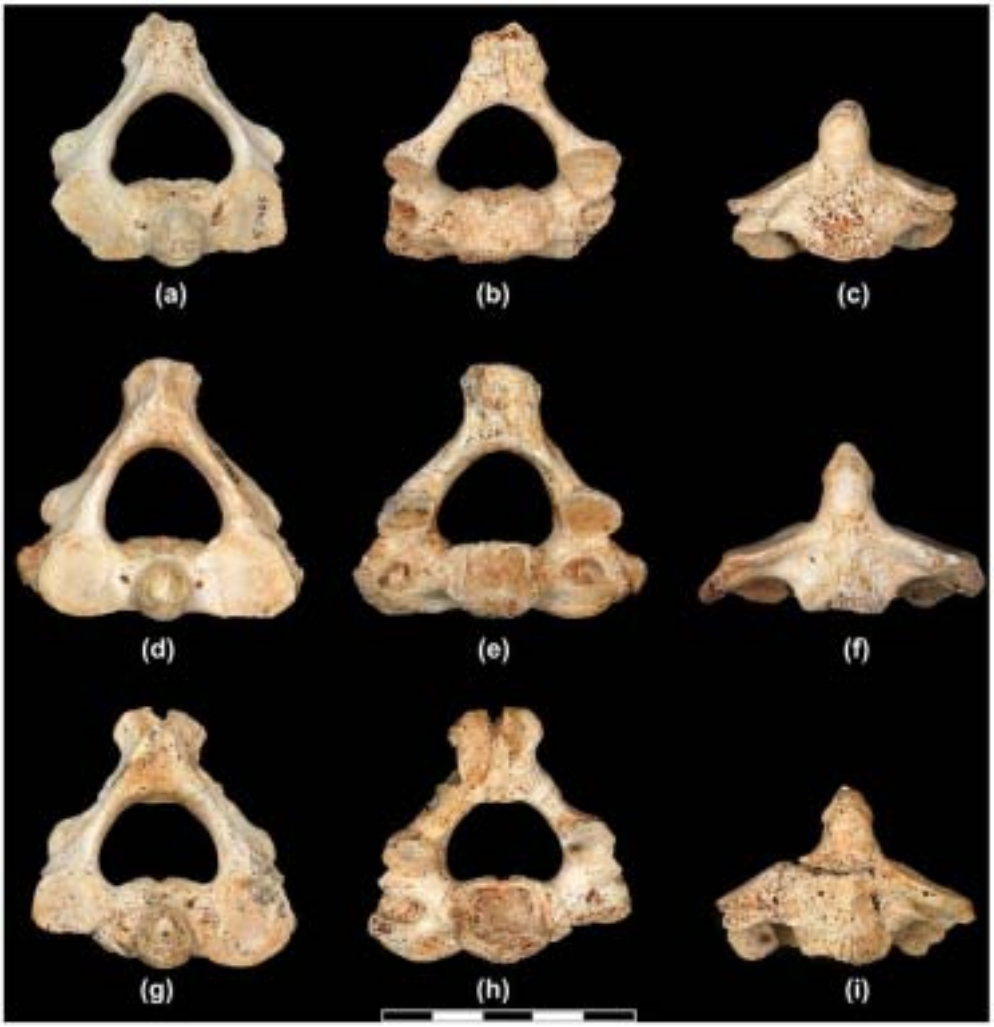

Fig. 4. Sima de los Huesos complete adult axes. VC2 axis in cranial (a), caudal (b), and ventral (c) views. VC4 axis in cranial (d), caudal (e), and ventral (f) views. VC8 axis in cranial (g), caudal (h), and ventral (i) views. Scale bar = 5 cm.

Size and shape of the vertebral foramen

The vertebral foramen of the atlas does not accurately reflect the size of the spinal cord (this trait will be discussed in the axis section and in the discussion below) because the ventral half is occupied by the dens of the axis. A Mann–Whitney *U*-test indicates that the SH sample has a significantly larger dorsoventral canal diameter (M10) than the Burgos modern human sample. The Neandertals have a larger canal, in both dorsoventral (M10) and transverse (M11) diameters, than the Burgos modern human sample. This larger dorsoventral diameter results in a high canal-shape index in Neandertals (Table 7), which could be related to the dorsoventral elongation of the foramen magnum, a proposed Neandertal autapomorphy (Rak et al., 1994, 1996; but see Creed-Miles et al., 1996). It appears that the length, rather than the shape of the foramen magnum, is primarily responsible for distinguishing Neandertals from modern humans (Rak et al., 1996).

The values for the dorsoventral diameter of the foramen magnum (M7) of SH crania are similar to those of Neandertals, and both of these values are significantly larger than those for our human male comparative samples (Table 8). Unfortunately, the number of associated fossil atlases and cranial bases is small. Figure 6 compares the dorsoventral diameter of the atlas with that of the foramen magnum in the VC7 atlas (associated with Cranium 5), La Ferrassie 1, Skhul V, Dolní Věstonice 14, Cro-Magnon, and two recent human samples. The SH specimen is well above the means for the modern human sample, but it is still inside their ranges. The fossil *H. sapiens* specimens from Skhul V and Cro-Magnon are just within the limits of the 95% equiprobability ellipse of the recent human samples. In contrast, the La Ferrassie 1 Neandertal and the Dolní Věstonice 14 modern human exhibit much larger values in both dimensions and are clearly outliers. When the variables are considered separately (Tables 6 and 8), the SH and Neandertal specimens lie between the recent human sample and the extreme La Ferrassie 1 individual.

The canal-shape index calculated for all the SH atlases is well within the recent human range of variation (Table 7). In contrast, the Neandertal mean canal-shape index is above the range of variation of the Burgos male sample, but it is still encompassed within the Hamann-Todd range of variation. When

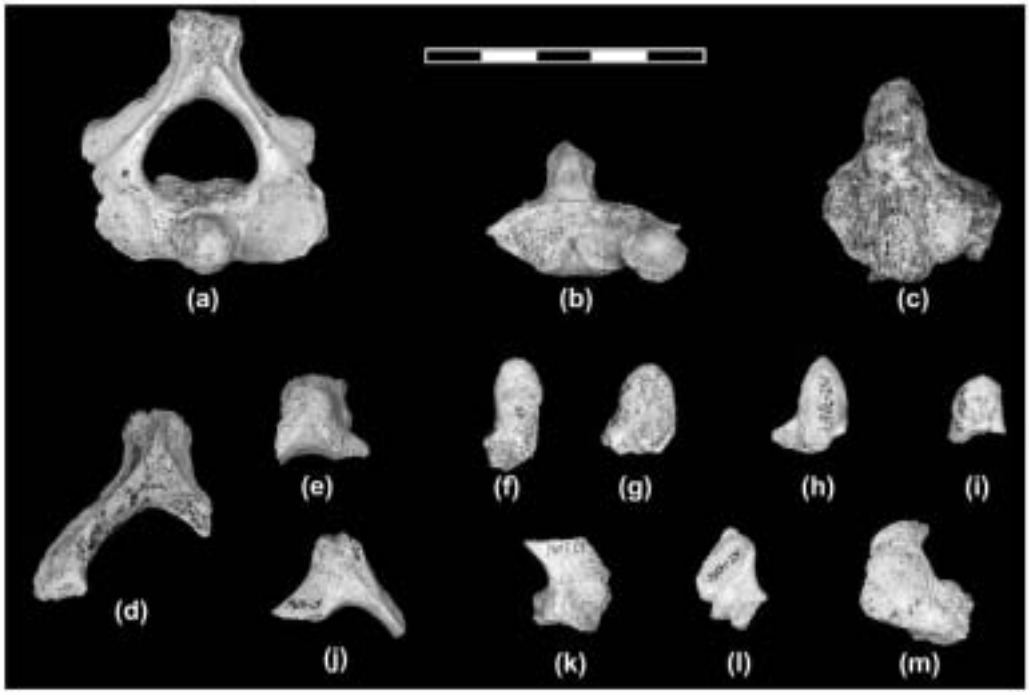

Fig. 5. Sima de los Huesos fragmentary and/or immature axes. (a) Cranial view of VC28. Dorsal views of (b) AT-1573 and (c) AT-2289. Cranial views of (d) AT-150 and (e) AT-4662. Ventral views of (f) AT-2883, (g) AT-3696, (h) AT-3979, and (i) AT-4314. Cranial views of (j) AT-4046, (k) AT-3741, (l) AT-4051, and (m) AT-4187. Scale bar = 5 cm.

Table 4
Sex assignments for Atapuerca (SH) and other fossil atlases and axes

	Sex assignment of individual	Atlas		Axis
		Sex using Marino's (1995) formulae[1]	Discriminant analysis[2] (sex; posterior probability)	Sex using Wescott's (2000) formulae[3]
VC3(C1), VC4(C2)		M (14)	M; 0.81	M (5/4)
VC7(C1), VC8(C2)		M (14)	M; 0.90	M (5/3)
VC16(C1), VC2(C2)		M (4)		M (5/5)
ATD6-90 (Gran Dolina)	F*	F (14)	F; 0.67	
Kebara 2	M†	M (8)		
Krapina 98		F (6)		
Krapina 104				F (1/1)
La Chapelle	M#	M(6)		
La Ferrassie 1	M**	M(14)	M; 0.78	M (5/5)
Régourdou 1	?			M (5/4)
Shanidar 2	M§	M (14)	M; 0.95	M (1/1)
Subalyuk 1	F¶	F (6)		
Percentage correct classification	—	75–85%	72.3%	81.7–83.4%

* Sex assignment is from Carretero et al. (1999).
† Sex assignment is from Rak and Arensburg (1987).
# Sex assignment is from Boule (1911–1913).
** Sex assignment is from Heim (1976).
? The sex of the Régourdou 1 specimen was undetermined by Vandermeersch and Trinkaus (1995), but discriminant analysis performed by Carretero (1994) on the clavicle sexed this individual as a male with a probability of 99%, and Churchill and Formicola (1997) considered it to be from a male in their analysis.
§ Sex assignment is from Trinkaus (1983).
¶ Sex assignment is from Pap et al. (1996).

[1] Marino (1995) proposed 14 different formulae (7 multiple regression equations and 7 discriminant functions). The number of these formulae that we have used is in parentheses. The formulae used different measurements, so the number of formulae used was contingent on the preservation of the fossil and/or the number of measurements available from the literature. All of the results were consistent with each other.

[2] Five variables were entered into the forward stepwise discriminant analysis (MDvD, STrD, ITrD, M10, M11); the variables used to calculate the discriminant function are: MDvD, STrD, ITrD.

[3] Wescott proposed five different discriminant equations. The number of formulae that we used and how many of them resulted in the proposed sex are in parentheses. Two equations in the case of VC8 and one in the case of VC4 and Régourdou 1 classified these specimens as females but with a result close to the sectioning point. In contrast, three of the formulae classified all of the SH specimens, La Ferrassie 1, and Régourdou 1 as males with a value well-above the mean for the male sample used by Wescott (2000).

Table 5
Raw dimensions (in mm) of the Sima de los Huesos atlases and results of the Mann–Whitney *U*-test for differences between sample means in SH, Neandertals, and recent humans

Variable	VC3	VC7	VC16	SH-N-BU	SH-BU		SH-N	BU-N	
				K-W	M-W	M-W (B)	M-W	M-W	M-W (B)
Maximum dorsoventral diameter (MDvD)#	47.4	48.1		*				*	†
Maximum transverse diameter (MTrD)	80.0								
Superior transverse diameter (STrD) §	49.7	51.5	(47.5)						
Inferior transverse diameter (ITrD) §	48.6	50.4	(48.3)	*	*	*			
Canal dorsoventral maximum diameter (M10)	34.8	33.3	(32.5)	**	*	†		**	*
Canal transverse maximum diameter (M11)	30.1	33.7	29.2						
Distance between the tubercles for the attachment of the transverse ligament (DTub)	18.6	20.3	16.5						
Anterior arch height at the level of the anterior tubercle (AAH)	10.5	12.2							
Anterior arch thickness at the level of the anterior tubercle (AATh)	6.6	6.3							
Transverse diameter of the facet for the axis (TrDFA)	11.8	11.8		**				*	*
Maximum height of lateral masses (MHLM)	19.5/20.0	22.6/22.6							
Posterior arch height at the level of the posterior tubercle (PAH)	8.5	9.3	9.5						
Posterior arch thickness at the level of the posterior tubercle (PATh)	5.9	7.6	7.6	*				*	†
Height of the posterior arch in the groove for the vertebral artery (HPAG)	4.1/5.5	—/5.3	4.3/4.9	X/**	/**	/*		/*	
Diameters in major axis of upper articular facets (UAFMAD)	22.7/22.1	(23.1)/24.7							
Diameters in right angle to major axis of upper articular facets (UAFTrD)	11.4/11.5	11.9/11.5		**/				*/	*/
Lower articular facet dorsoventral diameter (LAFDvD)	18.9/(18.0)	19.1/18.4	17.7/—	**/**	*/*	*/		**/**	*/*
Lower articular facet transverse diameter (LAFTrD)	15.9/15.4	16.0-16.5	16.1/—						

Values in parentheses are estimated. Cells that contain two entries are for the right and left sides (right/left).
Maximum anteroposterior diameter along the sagittal plane (McCown and Keith, 1939).
§ Maximum transverse diameter measured to the lateral margins of the superior or inferior articular facets (Trinkaus, 1983).
Abbreviations are as follows: SH = Sima de los Huesos; BU = Burgos males; N = Neandertals; HT = Hamann-Todd males; K-W refers to the Kruskal–Wallis test performed on SH, BU, and N samples; M-W refers to the Mann–Whitney *U*-test performed on different pairs of samples; M-W (B) refers to the Mann–Whitney *U*-test adjusted using the Bonferroni method; * $p < 0.05$; ** $p < 0.01$; † $0.05 < p < 0.10$; X = the analysis was not performed because one of the samples is of size $n = 0$ (K-W) or $n < 2$ (M-W).

Table 6
Comparison of linear atlas measurements (mm) between the SH specimens, Neandertals, and fossil and recent *H. sapiens*

	Sima de los Huesos			Neandertals[1]			Burgos males			H-T males	
	n	Mean	SD	*n*	Mean	SD	*n*	Mean	SD	Mean	SD
MDvD	2	47.8	0.5	2	50.9	3.3	35	44.8	2.8	46.6	3.3
MTRD	1	80.0					32	78.3	3.9	78.1	5.3
STrD	3	49.6	2.0	5	49.1	2.6	35	48.6	2.4	50.0	3.6
ITrD	3	49.1	1.1	5	47.5	2.0	36	45.5	2.5	46.4	2.7
M10	3	33.5	1.2	3	35.2	1.6	35	30.2	1.9	31.5	2.4
M11	3	31.0	2.4	5	30.1	2.2	36	29.0	2.1	28.5	2.4
DTub	3	18.5	1.9	2	17.3	1.5	36	16.0	2.0		
AAH	2	11.4	1.2	3	11.0	1.9	37	11.0	1.1	11.1	8.5
AATh	2	6.4	0.2	5	5.7	1.8	38	6.3	0.8	10.1	6.6
TrDFA	2	11.8	0.0	3	13.0	1.2	38	10.1	1.4		
MHLM	2/2	21.1/21.3	2.2/1.8	1/2	19.3/20.5	—/1.5	38/36	21.5/21.6	1.9/1.8		
PAH	3	9.1	0.5	2	8.2	2.5	35	9.9	2.0		
PATh	3	7.0	1.0	2	3.6	0.6	35	7.8	2.1		
HPAG	2/3	4.2/5.2	0.1/0.3	0/2	—/5.2	—/0.1	35/33	4.2/4.0	0.9/0.6		
UAFMAD	2/2	22.9/23.4	0.3/1.8	6/6	23.6/24.1	2.2/2.2	37/36	23.7/23.5	1.8/1.7		
UAFTrD	2/2	11.6/11.5	0.4/0.0	6/5	12.2/11.4	1.4/0.7	38/37	10.4/10.5	1.2/1.0		
LAFDvD	3/2	18.6/18.2	0.8/0.3	5/5	18.1/18.2	0.9/1.4	37/37	16.3/16.2	1.3/1.2		
LAFTrD	3/2	16.0/16.0	0.1/0.8	4/5	14.3/15.6	1.2/1.6	37/38	15.5/15.8	1.0/1.2		

Cells that contain two entries are for the right and left sides (right/left).
[1] Neandertal sample ($n = 9$; MNI = 8) includes: Kebara 2 (Arensburg, 1991); Krapina 98, 99, and 100; La Chapelle-aux-Saints; La Ferrassie 1; Shanidar 2; Subalyuk 1 (Pap et al., 1996); and Tabun C1 (McCown and Keith, 1939).

Table 7
Comparison of the indices of the atlas in the SH sample, Neandertals, and fossil and living *H. sapiens*

Specimen/sample	Shape index[1]	Canal-shape index[2]	Articular-facet superposition[3]
VC3	95.4	115.6	102.3
VC7	93.4	98.8	102.1
VC16	—	(111.3)	(98.3)
ATD6-90	89.1	111.1	102.0
Neandertals[4]	107.6 ± 1.4 (106.2–109.0) ($n = 2$)	118.4 ± 7.1 (106.0–127.4) ($n = 3$)	103.7 ± 6.1 (91.0–112.3) ($n = 5$)
Skhul V	96.6	98.4	99.8
Burgos (males)	92.3 ± 6.9 (77.9–107.5) ($n = 34$)	104.7 ± 7.8* (90.5–118.2) ($n = 35$)	107.1 ± 6.6 (93.3–121.4) ($n = 35$)
Hamann-Todd			
Males ($n = 50$)	93.6 ± 8.6 (74.6–117.6)	111.2 ± 9.0 (88.9–130.0)	107.8 ± 6.4 (92.2–121.9)
Females ($n = 51$)	92.7 ± 8.5 (75.0–116.0)	110.4 ± 9.4 (87.1–131.0)	108.0 ± 6.6 (96.9–127.2)
Total ($n = 101$)	93.2 ± 8.6 (74.6–117.6)	110.8 ± 9.2 (87.1–131.0)	107.9 ± 6.5 (92.2–127.2)

* Significantly different from Hamann-Todd sample ($p < 0.01$; Student's *t*-test).
[1] Shape-index = MDvD/STrD × 100.
[2] Canal-shape index = M10/M11 × 100.
[3] Articular-facet superposition = STrD/ITrD × 100.
[4] Neandertal sample includes: Kebara 2 (Arensburg, 1991), Krapina 98, La Ferrassie 1, Shanidar 2, and Subalyuk 1 (Pap et al., 1996).

the dorsoventral diameter of the canal is plotted against the transverse diameter (Fig. 7), the estimated values for Shanidar 2 fall out of the 95% equiprobability ellipse of the Hamann-Todd females and Burgos sample due to its extreme values. The three complete atlases from SH fall well within the 95% equiprobability ellipse of the Hamann-Todd male and Burgos male samples. Specimen VC7 falls outside the Hamann-Todd female subsample due to its large maximum transverse diameter of the canal (M11). Specimen ATD6-90 from Gran Dolina possesses small canal diameters, but it is still well-within our modern human samples' 95% equiprobability ellipses.

The area of the vertebral foramen of the most complete SH atlases is significantly larger ($p < 0.05$, Mann–Whitney *U*-test) than that of the Burgos male sample, regardless of the method used to estimate the area (Table 9). However, as noted above, this does not reflect the actual size of the spinal cord.

Tubercles for the insertion of the transverse ligament

The tubercles for the insertion of the transverse atlantal ligament are located just below the medial margin of each superior facet in the atlas (Gray, 1959). Tubbs et al. (2002) found that 14.7% of the tubercles in his sample ($n = 50$ individuals) "did not protrude from the lateral masses into the vertebral foramen and were merely smooth surfaces" (p. 345). Thus, we can recognize two different morphologies in the insertion of the transverse atlantal ligament: (1) a tubercle that protrudes into the vertebral foramen and (2) a flat surface or a tubercle significantly reduced in size that does not protrude into the vertebral foramen (Fig. 8). We will refer to the former morphology as "projected tubercle" or "large tubercle" and to the latter one as "weakly developed tubercle" or "small tubercle." We have classified the SH, Neandertal, and comparative samples into these two categories in Table 10. In the literature, the tubercles for the transverse ligament in Neandertals have been described as "slightly prominent" ("peu saillant"; Boule, 1911–1913: 92; Heim, 1976: 311), "small, poorly developed" (Arensburg, 1991:114), or even "replaced by a rough surface" ("remplacé par une surface rugueuse"; Martin, 1923: 214). These descriptions are fully consistent with the "small tubercle" morphology.

The first cervical vertebra ATD6-90 from Gran Dolina possesses a large tubercle for the attachment of the transverse ligament (Carretero et al., 1999; Gómez-Olivencia, 2005). We lack information about this trait for the left mass of the female *H. ergaster* specimen KNM-ER 1808 (Walker et al., 1982; Leakey and Walker, 1985) and for the left mass KNM-ER 1825, found at a locality where robust australopith fossils

Table 8
Comparison of the dorsoventral diameter of the foramen magnum in the SH sample, Neandertals, and recent humans[1]

Sample	Foramen magnum DV diameter (M7)	Reference
SH[2] ($n = 3$)	41.3 ± 3.1	Arsuaga et al., 1997c; Martínez, 1995
Neandertal pooled sex[3] ($n = 7$)	40.7 ± 4.7	Arsuaga et al., 1997c; Martínez, 1995; McCown and Keith, 1939; Present study
Burgos males ($n = 10$)	34.8 ± 1.7	Present study
Hamann-Todd males ($n = 22$)	36.3 ± 2.4	Present study
Coimbra males ($n = 78$)	36.8 ± 2.8	Martínez, 1995
Coimbra females ($n = 75$)	35.7 ± 2.6	Martínez, 1995

[1] The results of the Mann–Whitney *U*-test showed no significant difference between the SH and Neandertal samples, but both are significantly ($p < 0.05$ and $p < 0.01$, respectively) larger than the Burgos sample. The Coimbra males are significantly ($p < 0.05$) larger than the Coimbra females (Martínez, 1995).
[2] SH sample is composed of Crania 4, 5, and 6, all of which are assigned to male individuals.
[3] Neandertal sample includes: Gibraltar 1, La Chapelle-aux-Saints, La Ferrassie 1, Engis 2, Saccopastore 1, Shanidar 1, and Tabun C1.

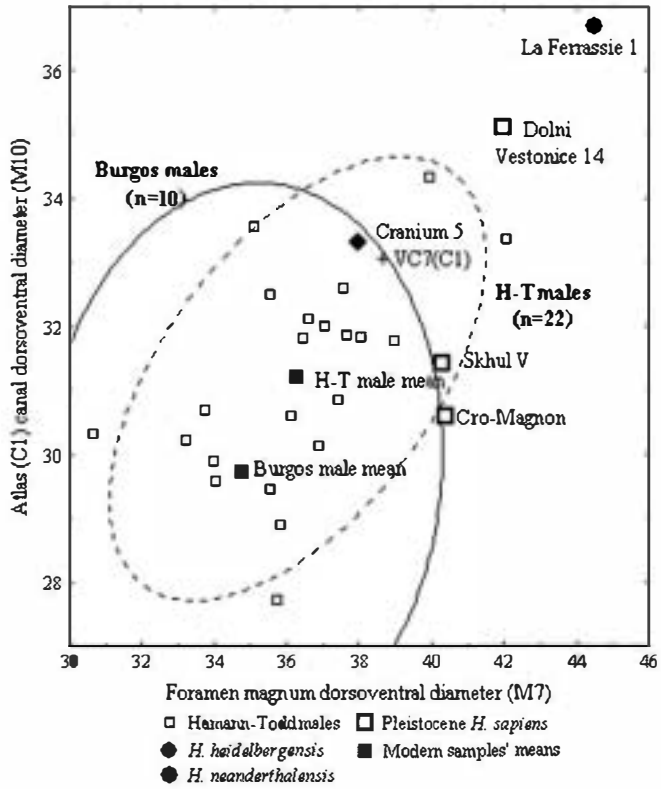

Fig. 6. Dorsoventral diameter of the foramen magnum versus the dorsoventral diameter of the atlas in several fossil specimens and recent humans. The 95% equiprobability ellipses for the Burgos male and the Hamann-Todd samples are shown.

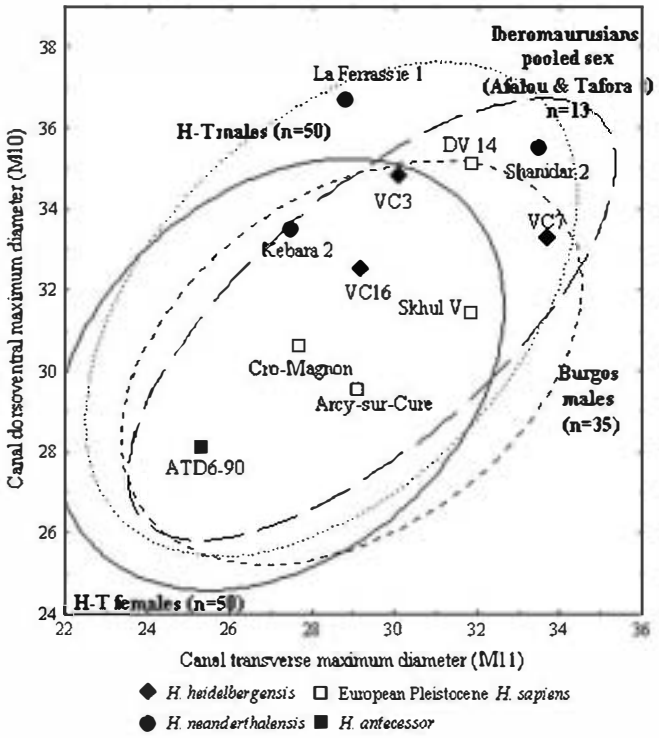

Fig. 7. Dorsoventral diameter of the canal vs. the maximum transverse diameter of the canal in the atlas in several fossil specimens, the terminal Pleistocene sample from the sites of Afalou and Taforalt, and several recent human samples. The 95% equiprobability ellipses are given for the Afalou/Taforalt and recent human samples. DV 14 refers to Dolní Věstonice 14.

have been collected (Leakey and Walker, 1985). The area in which the tubercles should be present has suffered mild damage to the left articular process of the *Australopithecus afarensis* atlas A.L. 333-83 (Lovejoy et al., 1982).

The atlases from the Sima de los Huesos site show higher frequencies of small tubercles than do our two modern human comparative samples, but lower frequencies than are observed in Neandertals. Although we cannot completely rule out the possibility that the condition is a general reflection of robusticity, the tubercle for the insertion of the transverse ligament does not appear to be remodeled by physical stress and thus the degree of development could be epigenetic (Tubbs et al., 2002), which implies that this trait could be useful as a phylogenetic character. Moreover, the percentages of small tubercles in the two modern human populations (Burgos and Afalou) are similar, despite their different chronology, geography, and lifestyles. The presence of large tubercles in the ATD6-90 atlas from Gran Dolina suggests that high frequencies of well-developed tubercles could be the primitive condition within the genus *Homo*, which has been preserved in late Pleistocene *H. sapiens*, as represented in the atlases SAM-AP 6268 from Klasies River Mouth (Grine et al., 1998) and Skhul V, and in the modern human samples (see above). In contrast, high frequencies of weakly developed tubercles would be the derived condition of *H. neanderthalensis*, and the middle Pleistocene European populations of *H. heidelbergensis* would represent an intermediate stage. Alternatively, we could hypothesize a polymorphic primitive condition that led to high frequencies of small tubercles in the European *H. heidelbergensis–H. neanderthalensis* lineage and to high frequencies of large tubercles in *H. sapiens*.

Table 9
Comparison of the vertebral-foramen area (mm^2) the SH and recent human atlases

Specimen/sample	Vertebral-foramen area 1*	Vertebral-foramen area 2**
VC3	726.7	697.3
VC7	781.6	749.7
VC16	(697.3)	(626.8)
Burgos[1] (males)	603.5 ± 63.2 (478.2–735.2) ($n = 30$)	594.6 ± 67.5 (458.7–723.9) ($n = 30$)

* Imaged area measures.

** Cross-checked for accuracy by comparing imaged linear measures to physical dimensions measured with digital calipers.

[1] The two mean values of the vertebral-foramen area in the Burgos sample are not statistically different.

Anterior tubercle of the anterior arch of the atlas

In the Sima de los Huesos atlases, all of the anterior arches ($n = 7$), regardless of their age at death, display a projecting anterior tubercle. The anterior tubercle of the anterior arch of the atlas (Fig. 9) projects caudally in 48.6% of the individuals in the modern human male comparative sample from Burgos

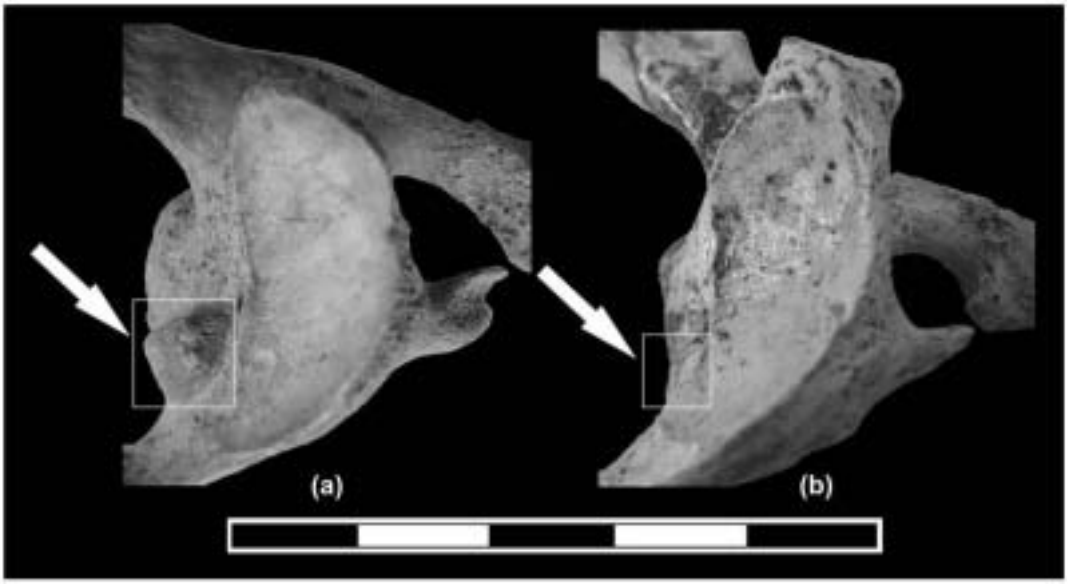

Fig. 8. Cranial view of the left mass of the atlas. (a) Modern human from the Burgos sample, showing a well-developed tubercle for the insertion of the atlantal transverse ligament, which protrudes medially into the vertebral foramen. (b) VC3 from SH showing a flat surface instead of a tubercle for the insertion of the atlantal transverse ligament.

($n = 37$). Among Neandertals, all of the atlases that preserve the anterior arch ($n = 5$) have anterior tubercles that clearly project caudally: La Quina (Martin, 1923), Kebara 2 (Arensburg, 1991), La Chapelle-aux-Saints (Boule, 1911–1913), La Ferrassie 1 (Heim, 1976), and Krapina 98 (Gorjanovic-Kramberger, in Boule, 1911–1913). A caudally projecting anterior tubercle of the atlas is also present in the Gran Dolina atlas ATD6-90 and the Klasies River Mouth atlas SAM-AP 6268 (Grine et al., 1998). In contrast, Skhul V does not possess this morphological pattern (McCown and Keith, 1939).

A caudally projecting anterior tubercle is not related to a thickened anterior arch in the SH sample. Moreover, the thickness of the anterior tubercle of VC3 and VC7 are similar to the mean value of our modern male comparative sample. The anterior tubercle is the insertion point of the longus colli muscle, which flexes the neck, so high frequencies of a caudal projection of the anterior tubercle could be related to the hypertrophy of this muscle.

Table 10
Comparison of the frequencies of weakly developed tubercles in the atlas of the SH specimens, Neandertals, and recent humans

Sample	Sex	Large tubercle	Asymmetry[1]	Small tubercle
SH[2] ($n = 6$)	Male ($n = 3$); unknown sex ($n = 3$)	33.3%	0%	66.7%
Neandertals[3] ($n = 6$)	Pooled sex	0%	16.7%	83.3%
Burgos ($n = 39$)	Male	74.4%	10.2%	15.4%
Afalou ($n = 12$)	Pooled sex	83.3%	0%	16.7%

[1] Asymmetry refers to the presence of a large tubercle in one of the lateral masses and a small tubercle in the other lateral mass of the atlas.

[2] Among the adult atlases from SH, the tubercles are large in VC16 and AT-3985 (MNI = 2) and are small in VC3, VC7, AT-1818, AT-2584, and AT-3013 (MNI = 4).

[3] Among Neandertals, the tubercles are weakly developed in La Ferrassie 1 (Heim, 1976; present study), La Chapelle (Boule, 1911–1913; present study), Kebara 2 (Arensburg, 1991), La Quina H5 (Martin, 1923), and Krapina 100 (present study). Shanidar 2 shows a large tubercle on the left side but a small one on the right side.

Posterior tubercle of the posterior arch of the atlas

The posterior tubercle of the posterior arch of the atlas is the insertion area for *M. rectus capitis posterior minor*, which extends (bilaterally) and rotates (unilaterally) the atlanto-occipital joint (Gray, 1959). In the three most complete individuals from SH, especially VC7, the posterior tubercle is big, and may be related to muscular hypertrophy.

Morphology and metrics of the axis

Metrics

The metric dimensions and indices of the SH axes and comparative data from Neandertal and modern samples are provided in Tables 11–13. Results of the Kruskal–Wallis test and Mann–Whitney *U*-test are given in Table 11; Table 12 compares Neandertal and modern samples to the SH sample.

The most remarkable feature of the SH axes is that they are relatively low (low value of M1a and DCCDA) and wide (high values of STrD) compared to our modern male samples (both recent and late Pleistocene), which are higher and narrower, as shown in Fig. 10. These differences result in lower shape and axis height/breadth indexes in the SH specimens. The SH axes clearly group with the Neandertals, but Skhul V also exhibits the same morphology, and so we cannot evaluate this trait phylogenetically. More fossils are needed to clarify this pattern.

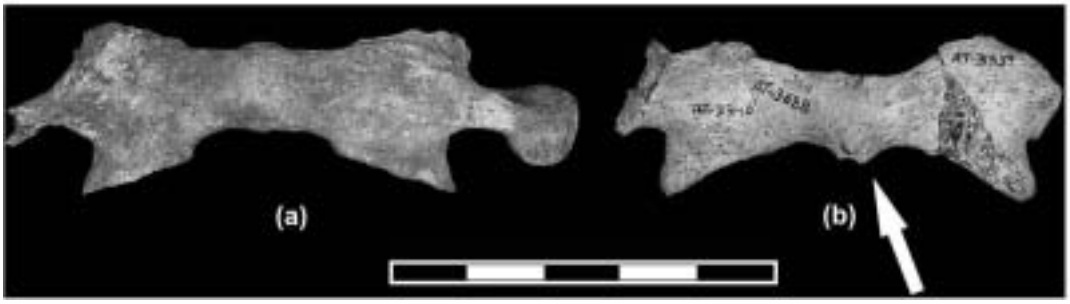

Fig. 9. (a) A modern atlas from the Burgos sample that lacks the anterior tubercle caudal projection. (b) Ventral view of VC7, showing the caudal projection of the anterior arch tubercle (arrow).

Size and shape of the vertebral foramen

The SH axes have canal-size dimensions and canal-shape indices that are well within our modern human sample range of variation (Tables 11–13; Fig. 11). Moreover, the area of the vertebral foramen calculated for the SH specimens is close to the mean of our Burgos male sample (Table 14). Among Neandertals, the remarkably large transverse diameter of the canal (M11) in Shanidar 2 and the large dorsoventral diameter of the canal (M10) in Krapina 105 place these vertebrae out of the 95% equiprobability ellipse of the modern human comparative sample from Burgos (Fig. 11).

Finally, we have compared the vertebral-canal surface area of the axes to their articular surface areas (as a proxy for size). The SH specimens' mean falls close to that of the Burgos human sample (Burgos mean = 97.9 ± 18.8, $n = 29$; SH mean = 99.6 ± 19.5, $n = 3$). Moreover, within the Burgos male sample, there is no evidence of a correlation between these two variables.

Pathological lesions

Pathology in the vertebral column has been described in several hominins (Cook et al., 1983; Dawson and Trinkaus, 1997; Trinkaus, 1985; Ogilvie et al., 1998), including some of the SH hominins (Pérez, 2003). We have found two kinds of pathology in the SH upper cervical vertebrae: a developmental defect and degenerative pathology.

In the VC3 atlas, the anterior bar of the transverse process remains unfused to the posterior bar of the transverse process, and thus the *foramen transversarium* is not completely delimited. The fusion of the anterior bar to the posterior bar of

Table 11
Raw dimensions (in mm) of the SH axes and results of the Mann–Whitney *U*-test for differences between sample means in SH, Neandertals, and recent humans

Variable	VC2	VC4	VC8	SH-N-BU	SH-BU		SH-N	BU-N	
				K-W	M-W	M-W(B)	M-W	M-W	M-W(B)
Maximum dorsoventral diameter (MDvD) #	(50.0)	50.1	48.9						
Maximum transverse diameter (MTrD) §		(60.0)							
Superior transverse diameter (STrD) §	(48.0)	50.5	51.1	**	**	*			
Inferior transverse diameter (ITrD)	46.0	(49.6)	45.4						
Canal dorsoventral maximum diameter (M10)	17.4	18.3	15.5						
Canal transverse maximum diameter (M11)	23.7	22.9	23.9	*				*	†
Body craniocaudal dorsal diameter (M2)	19.0	17.1	18.0	*				*	*
Total vertebral ventral height (M1a)	(34.5)	(36.2)	(36.0)	**	*			**	**
Total vertebral dorsal height (DoH)	31.5	32.2	31.9	*	*			*	
Body inferior anteroposterior diameter (M5)		(15.5)	(16.1)						
Body inferior transverse diameter (M8)	18.4	16.4	18.4						
Cranial articular facet dorsoventral diameter (UAFDvD)	17.0/17.7	16.1/17.0	—/18.2						
Cranial articular facet transverse diameter (UAFTrD)	19.2/—	15.9/15.1	—/19.6	/X					
Caudal articular facet dorsoventral diameter (LAFDvD)	10.4/—	10.0/—	11.9/10.9	/X					
Caudal articular facet transverse diameter (LAFTrD)	12.6/—	12.3/—	10.2/10.1	/X					
Laminae: craniocaudal diameter (CCDLam)	12.0/11.2	10.8/11.7	11.8/11.6	*/*				**/*	*/*
Laminae: thickness (ThLam)	4.9/4.5	5.8/6.6	5.2/7.0						
Spine length (M13)	(16.5)	17.0	18.4						
Maximum transverse diameter of the tip of the spinous process (TrDTSP)	12.8	(16.3)	18.5						

Values in parentheses are estimated. Cells that contain two entries are for the right and left sides (right/left).
Maximum anteroposterior diameter along the sagittal plane (McCown and Keith, 1939).
§ Maximum transverse diameter measured to the lateral margins of the superior or inferior articular facets (Trinkaus, 1983).
Abbreviations are as follows: SH = Sima de los Huesos; BU = Burgos males; N = Neandertals; HT = Hamann-Todd males; K-W refers to the Kruskal–Wallis test performed on SH, BU, and N samples; M-W refers to the Mann–Whitney *U*-test performed on different pairs of samples; M-W (B) refers to the Mann–Whitney *U*-test adjusted using the Bonferroni method; * $p < 0.05$; ** $p < 0.01$; † $0.05 < p < 0.10$; X = the analysis was not performed because one of the samples is of size $n = 0$ (K-W) or $n < 2$ (M-W).

Table 12
Comparison of linear axis measurements (mm) in the SH specimens, Neandertals, and fossil and recent *H. sapiens*

	Sima de los Huesos			Neandertals[1]			Burgos males			H-T males ($n = 50$)	
	n	Mean	SD	n	mean	SD	n	Mean	S.D	Mean	S.D
MDvD	3	49.7	0.7	4	51.2	4.0	35	49.6	2.3	51.6	2.8
MTRD	1	60.0	—	2	51.8	0.4	35	54.7	4.4	55.2	4.0
STrD	3	49.9	1.6	8	47.8	2.7	39	45.2	2.3		
ITrD	3	47.0	2.3	2	51.8	3.9	38	47.2	2.4	47.8	2.9
M10	3	17.1	1.4	6	18.0	1.6	39	16.5	1.5		
M11	3	23.5	0.5	8	24.5	1.3	39	23.1	1.3	23.4	1.9
M2	3	18.0	1.0	6	16.2	2.7	37	19.0	1.5		
M1a	3	35.6	0.9	9	34.3	2.8	38	37.9	2.3	38.9	2.6
DCCDA	3	31.9	0.4	5	30.7	3.2	38	34.0	2.1		
M5	2	15.8	0.4	7	16.2	2.1	39	15.1	1.1	16.7	1.6
M8	3	17.7	1.1	8	19.3	1.6	35	18.1	1.4	19.8	2.3
UAFDvD	2/3	16.6/17.6	0.6/0.6	3/2	17.9/18.3	1.1/3.0	37/39	17.7/18.1	1.2/1.4		
UAFTrD	2/2	17.6/17.3	2.3/3.1	1/0	15.0/—	—/—	36/39	16.4/16.3	1.3/1.4		
LAFDvD	3/1	10.8/10.9	1.0/—	2/0	11.8/—	0.6/—	36/35	10.1/10.1	1.4/1.4		
LAFTrD	3/1	11.7/10.1	1.3/—	2/0	12.4/—	0.2/—	35/34	11.2/11.2	1.2/1.5		
CCDLam	3/3	11.5/11.5	0.6/0.3	7/6	10.4/10.5	1.1/1.1	39	11.9/11.8	1.1/1.1		
ThLam	3/3	5.3/6.0	0.4/1.3	7/5	5.5/5.3	0.1/0.6	39	5.7/5.6	1.3/1.0		
M13	3	17.3	1.0	4	17.3	1.8	36	18.9	2.7		
TrDTSP	3	15.9	2.9	1	14.2	—	32	14.1	4.0		

Cells that contain two entries are for the right and left sides (right/left).

[1] The Neandertal sample ($n = 11$) comprises the following individuals: Kebara 2 (Arensburg et al., 1990; Arensburg, 1991), Krapina 103, Krapina 104, Krapina 105, La Chapelle-aux-Saints, La Ferrassie 1, La Quina H5 (Martin, 1923), Régourdou 1 (Piveteau, 1966), Shanidar 2, Shanidar 4 (Stewart, 1962; Trinkaus, 1983), and Tabun C1 (McCown and Keith, 1939).

the transverse process in modern humans occurs at about 3–4 years of age (Scheuer and Black, 2000).

The VC7 atlas shows a slight osteophytosis along the edges of its superior articular facets. This very slight osteophytosis finds its counterpart in the occipital condyles of Cranium 5, with which it is associated. Cranium 5's age at death has been estimated to be in excess of 35 years based on tooth wear, and thus it represents one of the oldest individuals in the SH sample, consistent with the appearance of this pathology. The VC16 atlas shows porosity in the middle-dorsal part of its superior articular facets. It exhibits abnormal proliferation of bone on the edge of the lower articular facet, which is congruent with the abnormal porous bone present on the associated VC2 axis at the edge of the superior articular facet. Moreover, the VC2 axis shows osteophytosis along the ventral edges of the superior articular facet (the only part of the facet that is preserved) and on the inferior articular facets. This would be consistent with early stages of degenerative joint disease (DJD). Finally, even if it cannot be considered technically pathological, the axis AT-2289 shows a rugosity on the craniolateral end of the dens on the alar ligament's insertion points. This condition could be related to a slight ossification of the ligamentous attachment point (enthesophyte).

In general, the level of DJD present in the SH upper cervical sample is not very severe, with the VC16-VC2 association being the most strongly affected. Degenerative joint disease is

Table 13
Comparison of the indices of the axis in the SH sample, Neandertals, and fossil and living *H. sapiens*

Specimen/sample	Shape index[2]	Canal-shape index[3]	Articular-facet superposition[4]	Axis height/width index[5]
VC2	(104.2)	73.4	(104.3)	(71.9)*
VC4	92.2*	79.9	(101.8)	(71.7)*
VC8	95.7*	64.9	112.6*	(70.5)*
Neandertals[1]	109.5 ± 11.3	73.8 ± 9.5	93.0 ± 1.9	$71.1^* \pm 8.3$
	(100.0–125.8) ($n = 4$)	(65.2–91.3) ($n = 6$)	(91.6–94.3) ($n = 2$)	(57.1–83.5) ($n = 8$)
Skhul V	107.0	69.3	—	67.6*
Burgos (males)	110.4 ± 5.6	70.9 ± 4.8	95.5 ± 4.5	84.1 ± 4.7
	(99.7–122.0) ($n = 35$)	(61.1–81.4) ($n = 36$)	(87.3–104.8) ($n = 37$)	(75.2–94.3) ($n = 38$)

Values in parentheses are estimated.

* Value is out of the Burgos recent human sample range.

[1] The Neandertal sample ($n = 8$) includes the following specimens: Kebara 2 (Arensburg et al., 1990; Arensburg, 1991), Krapina 103, Krapina 104, Krapina 105, La Chapelle-aux-Saints, La Ferrassie 1, Régourdou 1 (Piveteau, 1966), and Shanidar 2.

[2] Shape index = MDvD/STrD × 100.

[3] Canal-shape index = M10/M11 × 100.

[4] Articular-facet superposition = STrD/ITrD × 100.

[5] Axis height/width index = M1a/STrD.

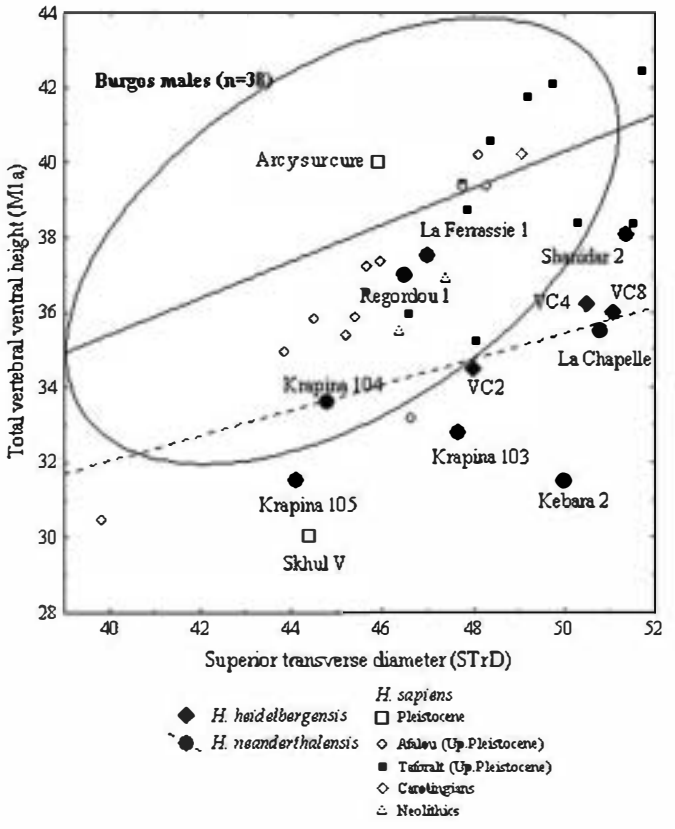

Fig. 10. Axis total vertebral height (y) vs. superior transverse diameter in the Burgos sample and several fossil atlases. The 95% equiprobability ellipse for the Burgos male sample and the regression line for the Burgos sample (solid line) and the Neandertals (dotted line) are shown. For the Burgos modern male sample, $y = 0.4879x + 15.8829$ ($n = 38$). For the Neandertal sample, $y = 0.3415x + 18.369$ ($n = 8$). The extremely low value for the total vertebral height in the Kebara 2 axis could be due to an underestimation of this measurement by Arensburg et al. (1990). On the other hand, McCown and Keith (1939) underscore the smallness of Skhul V axis.

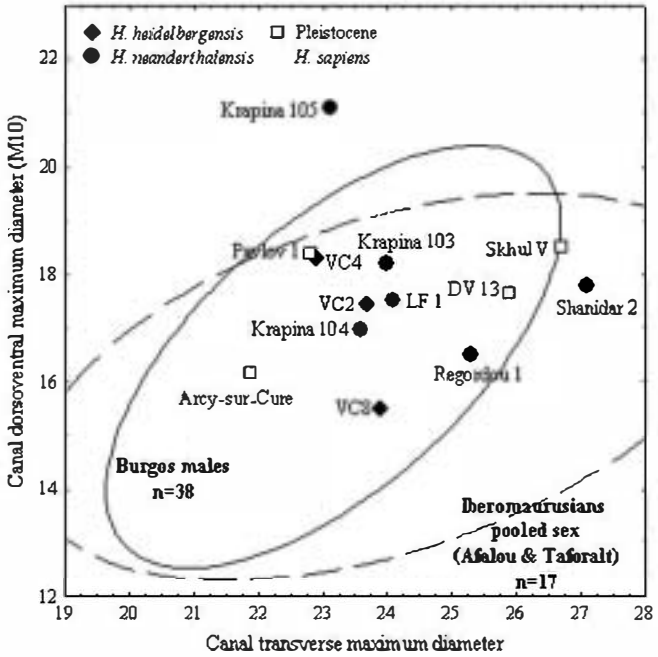

Fig. 11. Axis canal dorsoventral diameter (y) vs. canal transverse maximum diameter in the Burgos sample and several fossil atlases. The 95% equiprobability ellipses for the Burgos male sample and for the Iberomaurusian pooled sex sample are given. DV 13 refers to Dolní Věstonice 13. LF1 refers to La Ferrassie 1. The value of M10 reported by McCown and Keith (1939) for the Skhul V axis is 24.6 mm, 0.1 mm above the value reported by Stewart (1962), which is 6 mm above our value. This extraordinary difference could be due to differences in measurement method (see Fig. 1).

age-progressive (Aufderheide and Rodríguez-Martín, 1998). In 80% of the cases, no cause is evident, and in other cases, the cause may be physical, infectious, or metabolic, among other factors.

Bocquet-Appel and Arsuaga (1999) demonstrated that there is a dearth of mature adult individuals at the SH site. Based on the study of dental wear, Bermúdez de Castro et al. (2004) found only three individuals who were older than 35 years (one male and two of indeterminate sex). Of these three individuals, one could also be represented by Pelvis 1 (older than 35) and another, represented by the isolated pubis AT-2500, could be more than 45 years.

Bermúdez de Castro and Pérez (1995) studied the enamel hypoplasia in the SH sample to determine the level of biological stress that affected the development of these hominins. They found that this population probably suffered a lower level of biological stress than did Neandertal populations (see also Cunha et al., 2004).

In summary, the appearance of different degrees of DJD in two SH adult individuals represented by the upper cervical vertebrae could indicate that these vertebrae belong to some of the older individuals represented by the dental material. In one case, this is confirmed by the association of VC7(C1) and VC8(C2) with Cranium 5 (age at death ≥ 35; Bermúdez de Castro et al., 2004).

Discussion

Phylogenetic evidence suggests that the SH sample and all European middle Pleistocene hominins represent populations that were ancestral to the Neandertal populations, as they are characterized by a mixture of shared primitive features and Neandertal apomorphies (Arsuaga et al., 1997c; Carretero

Table 14
Comparison of the vertebral-foramen area (mm^2) of the SH and recent human axes

Specimen/sample	Vertebral-foramen area 1*	Vertebral-foramen area 2**
VC2	(306.3)	(302.0)
VC4	329.1	331.4
VC8	295.4	314.0
Burgos[1] (males)	301.9 ± 43.1 (234.5–401.2) ($n = 30$)	302.9 ± 47.5 (233.8–415.2) ($n = 30$)

Values in parentheses are estimated.
* Imaged linear measures.
** Cross-checked for accuracy by comparing imaged linear measures to physical dimensions measured with digital calipers.
[1] The two mean values of the vertebral-foramen area in the Burgos sample are not statistically different.

et al., 1997; Martínez and Arsuaga, 1997). In the SH upper cervical vertebral sample, we have found some features that could be of phylogenetic significance but whose polarity is difficult to ascertain due to the scarcity of hominin vertebrae. Within this group we can mention: (1) the development of the tubercle for the attachment of the transverse ligament of the atlas and (2) the height/breadth index of the axis. We should note that the SH specimens are metrically more similar to Neandertals than to our modern human comparative samples. Moreover, we have found that (1) the atlases from the Sima de los Huesos site exhibit a percentage of weakly developed tubercles for the attachment of the transverse ligament that is intermediate between modern human populations and Neandertals, and (2) the SH axes exhibit a height/breadth index similar to that of the Neandertals. These findings are fully compatible with the phylogenetic position proposed for these hominins (i.e., that *H. heidelbergensis* is an exclusively European species, ancestral only to *H. neanderthalensis*; Arsuaga et al., 1997c; Carretero et al., 1997; Martínez and Arsuaga, 1997).

Biomechanics

The atlanto-occipital articulation allows only for flexion and extension (Bogduk and Mercer, 2000). It acts as a first-class lever in which the occipital condyles act as the fulcrum, lying between the nuchal muscles and the mass of the head (Escuredo et al., 2002). In all other respects, the head and atlas move essentially as a single unit. Few muscles act directly on the atlas and, in fact, its movements are governed by the muscles that act on the head (Bogduk and Mercer, 2000). The SH hominins show a degree of prognathism (as measured by basion–prosthion length) that is similar to that of the Neandertals (Arsuaga et al., 1997c) and well-above the prognathism of modern humans (Martínez, 1995). The SH atlases show enlarged insertion areas for *M. rectus capitis posterior minor* and the SH axes have robust spinous processes that could relate to development of *M. obliquus capitis inferior* and *M. rectus capitis posterior major*. While these features could indicate muscular force acting at the atlanto-occipital joint to counter the aforementioned prognathism, we should recall that other muscles also act to extend the head (e.g., the *M. semispinalis capitis*), which could also play an important biomechanical role in this joint. Alternatively, these enlarged muscular-attachment areas could simply reflect a generally robust body build and/or high activity levels, factors that could produce increased caudal projection of the anterior tubercle, which would agree with the high body mass calculated for these hominins (Arsuaga et al., 1999; Carretero et al., 2004).

The upper cervical spine of the SH hominins is characterized by a mediolaterally expanded atlantoaxial joint, represented by the ITrD of the atlas and the STrD of the axis, and a short craniocaudal dimension of the axis. During lateral inclination of the head, there is no movement in the atlantoaxial joint (Kapandji, 1998) and we hypothesize that a mediolateral expansion would further stabilize this joint. The close relationship between neck biomechanics and head movement and the fact that the head is the final link in an open kinematic chain that includes the cervical and the upper thoracic vertebrae (Winters and Peles, 1990) make it necessary, if we want to fully assess the biomechanics of this anatomical region, to take into account both the upper and lower cervical vertebrae and cranial morphology, which we plan to do in a future publication.

Size of the vertebral canal and its implications

Much attention has been devoted to vertebral-canal size and its relationship to spoken language. One factor in the evolution of human language that would be reflected in vertebral-canal morphology is increased breath control (MacLarnon, 1993; MacLarnon and Hewitt, 1999, 2004). Modern humans have an enlarged thoracic vertebral canal, reflecting a larger amount of gray matter. Based on the morphology of the KNM-WT 15000 individual, a narrower thoracic canal has been proposed for *Homo ergaster*, indicating that this species may only have been capable of short, unmodulated utterances, such as those used by extant nonhuman primates (MacLarnon and Hewitt, 1999). However, significant abnormalities have been found in the KNM-WT 15000 individual (Latimer and Ohman, 2001), which could indicate some form of axial dysplasia, and so the small canal may be a reflection of a neural-canal stenosis associated with the pathology. In contrast, Schiess et al. (2006) argued that the diagnosis of a congenital dysplasia is not supported, indicating that the pathological lesions in the KNM-WT 15000 individual may not be as severe as previously reported. Moreover, the Dmanisi vertebrae (Meyer, 2005; Meyer et al., 2006), which are the oldest known for the genus *Homo*, follow the modern human pattern in all regions, as the raw and relative sizes of the vertebral canals fall well within the human range, indicating that these hominins may have had fine control of the respiratory muscles involved in spoken language (Meyer, 2005; Meyer et al., 2006).

Arsuaga et al. (1997a) showed that the mean cranial capacity of SH's three most complete crania (1245 cm^3) (Arsuaga et al., 1993, 1997c) is slightly less than that of two comparative samples from the Hamann-Todd Osteological Collection. However, given the large body-weight estimates for these hominins, their encephalization quotients are below both modern human or Neandertal values (Arsuaga et al., 1999). In Neandertals, higher encephalization quotients are reached by expansion of the cranial capacity, while in modern humans it is mainly achieved by a reduction in body mass (Arsuaga et al., 1999; Carretero et al., 2004). In addition to the parallel trends in encephalization in these two lineages, the absolute size of the bony vertebral canal in the upper cervical spine reached modern human values by the middle Pleistocene. Preliminary studies (Carretero et al., 1999; Gómez et al., 2004; Gómez-Olivencia, 2005) have shown that the SH lower cervical spine's canal had a similar size compared to modern humans, but a full assessment of this anatomical region will not be possible until larger sets of cervical and thoracic vertebrae are associated. In any case, as demonstrated by Martínez et al. (2004), the SH hominins had the skeletal characteristics of the outer and middle ear that support the perception of spoken language.

Summary and conclusions

Study of the SH upper cervical spine leads us to identify a minimum of 11 individuals represented by these fossils: 6 adults and 5 subadults. Three sets of associated atlases and axes, probably belonging to male individuals, have been identified: two older adults (one of them associated with Cranium 5) and one young adult. Metrical and morphological attributes reveal that SH atlases and axes are more similar to Neandertal homologues than to our modern male comparative samples. The SH upper cervical spine is characterized by: (1) a large maximum dorsoventral diameter of the atlas's canal, which may be related to the large dorsoventral diameter of the foramen magnum; (2) dorsoventrally large lower facets of the atlas; (3) a mediolaterally expanded atlantoaxial joint; (4) a craniocaudally short axis; (5) a caudally projecting anterior tubercle of the anterior arch of the atlas; and (6) lateral masses of the atlas that possess weakly developed tubercles for the attachment of the transverse ligament at frequencies that lie between those of modern humans and Neandertals. Future associations of more cervical elements from SH will clarify the anatomy of this region and will improve our understanding of the biology of these humans.

Acknowledgements

Special thanks go to our colleagues and friends A. Gracia, C. Lorenzo, N. García, R. Quam, and A. Esquivel for their great work at the Sima de los Huesos site. M.C. Ortega restored the fossils for us. We are grateful to Jakov Radovcic (Croatian Natural History Museum), Bruce Latimer and Yohannes Haile-Selassie (Cleveland Natural History Museum), Philippe Mennecier (Musée de l'Homme), Dominique Grimaud-Hervé (Département de Préhistoire—Muséum national d'Histoire naturelle), José María Bermúdez de Castro (Centro de Investigación de Evolución Humana), Belen Castillo (Museo de Burgos), and Michele Morgan (Peabody Museum of Archaeology and Ethnology) for providing access to the skeletal collections in their care. We are also indebted to Aurélie Fort, Lyman Jellema, Stéphanie Renault, and Olivia Herschensohn for curatorial assistance. Further thanks go to our colleagues at the Laboratorio de Evolución Humana (LEH) of the Universidad de Burgos and at the Centro UCM-ISCIII de Investigación sobre Evolución y Comportamiento Humanos. Special thanks go to Aimara for her help in the determination of the vertebral-canal area, with the figures, and all her comments, which greatly improved this manuscript. Luis Cabo provided helpful advice regarding statistics. Antoine Balzeau, Isabelle de Groote, J.E. González Urquijo, and Jeremiah Scott provided helpful comments on different parts of the manuscript. We are indebted to Marc R. Meyer discussing ideas dealing with vertebrae. We are grateful to Rolf Quam and Ciarán Brewster (P.D.), who helped with the English translation. Angelica Torres kindly revised the English in an earlier version of the manuscript. Rolf Quam also provided helpful comments that greatly improved this paper. We are indebted to William H. Kimbel for his thorough edit of the manuscript and his helpful comments, as well as those provided by the associate editor and three anonymous referees, which greatly improved the manuscript.

The first author is supported by a grant from the Ministerio de Educación y Ciencia. Laura Rodríguez is supported by a grant from the Fundación Siglo para las Artes en Castilla y León. This research was supported by the Ministerio de Ciencia y Tecnología, Proyecto BOS2003-08938-C03-01. Funding for the fieldwork came from the Junta de Castilla y León and Fundación Atapuerca. Help in the field from the Grupo Espeleológico Edelweiss was essential.

Appendix 1. Labeling of the SH vertebrae

Every human fossil from this site is identified by the field label "AT-" followed by the inventory number. For example, AT-333 is a distal epiphysis of a left adult humerus (see Carretero et al., 1997) and AT-121 is a frontal bone (Arsuaga et al., 1991). The fossils that consist of several fragments and labels have a second identification number with the initial letter of the bone and a Roman numeral. For example, H-I is Humerus I, a distal epiphysis of an immature individual composed of AT-741 and AT-791 (Carretero et al., 1997). In the case of anatomical parts that consist of different bones, like crania, a third inventory number is used. When significant parts of the calvaria (including different bones) are represented (with or without the face), the term "cranium" is used to label it, followed by an Arabic number. For example, Cranium 1 comprises AT-40, AT-63a-b, AT-65, AT-86, AT-122, AT-177a-e, AT-206, AT-216, AT-223, AT-472, and AT-937 (Arsuaga et al., 1997c), which includes Occipital IX [described as an isolated cranial bone by Arsuaga et al. (1991)]. Finally, based on dental evidence, 28 individuals have been identified (Bermúdez de Castro et al., 2004) and are labeled with Roman numerals. For example, the individual XXI includes Cranium 5 and the mandible AT-888.

We present a somewhat different way of labeling the SH vertebrae from that used for other bones in the same collection due to the large number of vertebral elements within each spine and the difficulty in assessing the exact anatomical position of vertebrae in some cases. The most complete vertebrae are also labeled with a "V" (for vertebra) and the initial letter of the vertebral region to which they belong ("C" for cervical, "T" for thoracic, and "L" for lumbar). Arabic numbers indicate the "inventory" number within each vertebral region. For example, VC16 is formed by AT-1140 and AT-2201, and among the most complete cervical vertebrae, it is the sixteenth labeled element (Table 2). Specimen VC15 is formed only by AT-2582, but this vertebra is complete enough to warrant a VC label, and among the most complete cervical vertebrae, it is the fifteenth labeled element. To make the discussion in the text easier to follow, the anatomical position within the region is indicated in parentheses. For example, VC1(C7) (formerly known as C7-I in Carretero et al., 1999) is formed by AT-321, AT-1556, AT-1569, and AT-1609, and it is the first labeled cervical of the sample (Table 2); the specimen is a seventh

cervical vertebra. Specimen VT27(T4-8) is formed by AT-1135 and AT-4008 and is the twenty-seventh thoracic element labeled, and its anatomical position lies between the fourth and the eighth thoracic vertebrae. For other elements, even if the anatomical determination can be made with complete accuracy we use the "AT-" field label due to the incompleteness of the fossil. For example, AT-2883 is the dens of an axis (C2) (Table 3). Future reconstructions of "AT-" labeled fragments will yield new complete VC specimens.

References

Arensburg, B., 1991. The vertebral column, thoracic cage and hyoid bone. In: Bar-Yosef, O., Vandermeersch, B. (Eds.), Le squelette moustérien de Kébara 2. Éditions du CNRS, Paris, pp. 113–147.

Arensburg, B., Schepartz, L.A., Tillier, A.M., Vandermeersch, B., Rak, Y., 1990. A reappraisal of the anatomical basis for speech in Middle Palaeolithic hominids. Am. J. Phys. Anthropol. 83, 137–146.

Arsuaga, J.L., Carretero, J.M., Lorenzo, C., Gracia, A., Martínez, I., Bermúdez de Castro, J.M., Carbonell, E., 1997a. Size variation in middle Pleistocene humans. Science 277, 1086–1088.

Arsuaga, J.L., Martínez, I., Gracia, A., Carretero, J.M., Lorenzo, C., Garcia, N., Ortega, A.I., 1997b. Sima de los Huesos (Sierra de Atapuerca, Spain). The site. J. Hum. Evol. 33, 109–127.

Arsuaga, J.L., Martínez, I., Gracia, A., Lorenzo, C., 1997c. The Sima de los Huesos crania (Sierra de Atapuerca, Spain). A comparative study. J. Hum. Evol. 33, 219–281.

Arsuaga, J.L., Carretero, J.M., Martínez, I., Gracia, A., 1991. Cranial remains and long bones from Atapuerca/Ibeas (Spain). J. Hum. Evol. 20, 191–230.

Arsuaga, J.L., Lorenzo, C., Carretero, J.M., Gracia, A., Martínez, I., García, N., Bermúdez de Castro, J.M., Carbonell, E., 1999. A complete human pelvis from the middle Pleistocene of Spain. Nature 399, 255–258.

Arsuaga, J.L., Martínez, I., 2004. Atapuerca y la Evolución Humana. Fundació Caixa Catalunya, Barcelona.

Arsuaga, J.L., Martínez, I., Gracia, A., Carretero, J.M., Carbonell, E., 1993. Three new human skulls from the Sima de los Huesos middle Pleistocene site in Sierra de Atapuerca, Spain. Nature 362, 534–537.

Aufderheide, A.C., Rodríguez-Martín, C., 1998. The Cambridge Encyclopedia of Human Paleopathology. Cambridge University Press, Cambridge.

Bermúdez de Castro, J.M., Pérez, P.J., 1995. Enamel hypoplasia in the middle Pleistocene hominids from Atapuerca (Spain). Am. J. Phys. Anthropol. 96, 301–314.

Bermúdez de Castro, J.M., Martinón-Torres, M., Lozano, M., Sarmiento, S., Muela, A., 2004. Paleodemography of the Atapuerca–Sima de los Huesos hominin sample: a revision and new approaches to the paleodemography of the European middle Pleistocene population. J. Anthropol. Res. 60, 5–26.

Bischoff, J.L., Shamp, D.D., Aramburu, A., Arsuaga, J.L., Carbonell, E., Bermúdez de Castro, J.M., 2003. The Sima de los Huesos hominids date to beyond U/Th equilibrium (>350 kyr) and perhaps to 400–500 kyr: new radiometric dates. J. Archaeol. Sci. 30, 275–280.

Bischoff, J.L., Williams, R.W., Rosenbauer, R.J., Aramburu, A., Arsuaga, J.L., García, N., Cuenca-Bescós, G., 2006. High-resolution U-series dates from the Sima de los Huesos hominids yields 600 $+\infty/-66$ kyrs: implications for the evolution of the early Neanderthal lineage. J. Archaeol. Sci. 34, 763–770.

Boaz, N.T., Ciochon, R.L., Xu, Q., Liu, J., 2004. Mapping and taphonomic analysis of the *Homo erectus* loci at Locality 1 Zhoukoudian, China. J. Hum. Evol. 46, 519–549.

Bocquet-Appel, J.P., Arsuaga, J.L., 1999. Age distributions of hominid samples at Atapuerca (SH) and Krapina could indicate accumulation by catastrophe. J. Archaeol. Sci. 26, 327–338.

Bogduk, N., Mercer, S., 2000. Biomechanics of the cervical spine. I: Normal kinematics. Clin. Biomech. 15, 633–648.

Boule, M., 1911–1913. L'homme fossile de la Chapelle-aux-Saints. Ann. Paléontol. 6, 111–172. 7, 21–56, 85–192; 8, 1–70.

Bräuer, G., 1988. Osteometrie. In: Knussmann, R. (Ed.), Anthropologie. Handbuch der vergleichenden Biologie des Menschen. Gustav Fischer, Stuttgart, pp. 160–232.

Buikstra, J.E., Gordon, C.C., St. Hoyme, L., 1984. The case of severed skulls. Individuation in forensic anthropology. In: Rathbun, T., Buikstra, J.E. (Eds.), Human Identification: Case Studies in Forensic Anthropology. Charles C. Thomas Pub. Ltd., pp. 121–135.

Carbonell, E., Mosquera, M., Ollé, A., Rodríguez, X.P., Sala, R., Vergés, J.M., Arsuaga, J.L., Bermúdez de Castro, J.M., 2003. Les premiers comportements funéraires auraient-ils pris place à Atapuerca, il y a 350 000 ans? L'Anthropologie 107, 1–14.

Carretero, J.M., 1994. Estudio del esqueleto de las dos cinturas y el miembro superior de los homínidos de la Sima de los Huesos, Sierra de Atapuerca, Burgos. Ph.D. Dissertation, Universidad Complutense de Madrid.

Carretero, J.M., Arsuaga, J.L., Lorenzo, C., 1997. Clavicles, scapulae and humeri from the Sima de los Huesos Site (Sierra de Atapuerca, Spain). J. Hum. Evol. 33, 357–408.

Carretero, J.M., Arsuaga, J.L., Martínez, I., Quam, R., Lorenzo, C., Gracia, A., Ortega, A.I., 2004. Los humanos de la Sima de los Huesos (Sierra de Atapuerca) y la evolución del cuerpo en el género *Homo*. In: Baquedano, E., Rubio, S. (Eds.), Miscelánea en Homenaje a Emiliano Aguirre. Volumen III. Paleoantropología. Museo Arqueológico Regional, Alcalá de Henares, pp. 120–135.

Carretero, J.M., Lorenzo, C., Arsuaga, J.L., 1999. Axial and appendicular skeleton of *Homo antecessor*. J. Hum. Evol. 37, 459–499.

Churchill, S.E., Formicola, V., 1997. A case of marked bilateral asymmetry in the upper limbs of an Upper Palaeolithic male from Barma Grande (Liguria), Italy. Int. J. Osteoarchaeol. 7, 18–38.

Cook, D.C., Buikstra, J.E., DeRousseau, C.J., Johanson, D.C., 1983. Vertebral pathology in the Afar australopithecines. Am. J. Phys. Anthropol. 60, 83–102.

Creed-Miles, M., Rosas, A., Kruszynski, R., 1996. Issues in the identification of Neandertal derivative traits at early post-natal stages. J. Hum. Evol. 30, 147–153.

Cuenca-Bescós, G., Laplana, C., Canudo, J.I., Arsuaga, J.L., 1997. Small mammals from Sima de los Huesos. J. Hum. Evol. 33, 175–190.

Cunha, E., Ramirez Rozzi, F.V., Bermudez de Castro, J.M., Martinón-Torres, M., Wasterlain, S.N., Sarmiento, S., 2004. Enamel hypoplasias and physiological stress in the Sima de los Huesos middle Pleistocene hominins. Am. J. Phys. Anthropol. 125, 220–231.

Dawson, J.E., Trinkaus, E., 1997. Vertebral osteoarthritis of the La Chapelle-aux-Saints 1 Neanderthal. J. Archaeol. Sci. 24, 1015–1021.

Escuredo, B., Sánchez, J.M., Borrás, F.X., Serrat, J., 2002. Estructura y función del cuerpo humano. McGraw-Hill, Interamericana, Madrid.

García, N., 2002. Los carnívoros de los yacimientos Pleistocenos de la Sierra de Atapuerca. Ph.D. Dissertation, Universidad Complutense de Madrid.

García, N., Arsuaga, J.L., Torres, T., 1997. The carnivore remains from the Sima de los Huesos middle Pleistocene site (Sierra de Atapuerca, Spain). J. Hum. Evol. 33, 155–174.

Gómez, A., Carretero, J.M., Arsuaga, J.L., Martínez, I., Quam, R., Lorenzo, C., Gracia, A., García, N., Ortega, A.I., Rodríguez, L., 2004. El raquis de los humanos del yacimiento de la Sima de los Huesos (Sierra de Atapuerca, Burgos). In: Egocheaga, J.E. (Ed.), Biología de Poblaciones Humanas: Diversidad, Tiempo, Espacio. Dpto. de Biología de Organismos y Sistemas, Antropología Física, Universidad de Oviedo, Oviedo, pp. 283–293.

Gómez, A., Carretero, J.M., Rodríguez, L., García, R., Arsuaga, J.L., 2005. The cervical vertebrae from the Sima de los Huesos site (Sierra de Atapuerca, Burgos, Spain). Am. J. Phys. Anthropol. 40 (Suppl.), 107.

Gómez-Olivencia, A., 2005. Estudio de la columna cervical de los humanos de la Sima de los Huesos (Sierra de Atapuerca, Burgos). Master's Thesis, Universidad Complutense de Madrid.

Gray, H., 1959. Anatomy of the Human Body. Lea and Febiger, Philadelphia.

Grine, F.E., Pearson, O.M., Klein, R.G., Rightmire, G.P., 1998. Additional human fossils from Klasies River Mouth, South Africa. J. Hum. Evol. 35, 95–107.

Heim, J.-L., 1976. Les Hommes fossiles de la Ferrassie. I. Le Gisement. Les Squelettes Adultes (Crâne et Squelette du Tronc). Masson, Paris.

Holliday, T.W., 2006. The vertebral columns. In: Trinkaus, E., Svoboda, J. (Eds.), Early Modern Human Evolution in Central Europe. Oxford University Press, Oxford, pp. 242–294.

Irish, J.D., 2000. The Iberomaurusian enigma: North African progenitor or dead end? J. Hum. Evol. 39, 393–410.

Kapandji, A.I., 1998. Fisiología Articular. 3. Tronco y Raquis. Editorial Médica Panamericana. Maloine, Madrid.

Latimer, B., Ohman, J.C., 2001. Axial dysplasia in *Homo erectus*. J. Hum. Evol. 40, A12.

Leakey, R.E.F., Walker, A.C., 1985. Further hominids from the Plio-Pleistocene of Koobi Fora, Kenya. Am. J. Phys. Anthropol. 67, 135–163.

Leroi-Gourhan, A., 1958. Étude des restes humains fossiles provenant des grottes d'Arcy-sur-Cure. Ann. Paléontol. 44, 87–148.

Lovejoy, C.O., Johanson, D.C., Coppens, Y., 1982. Elements of the axial skeleton recovered from the Hadar formation: 1974–1977 collections. Am. J. Phys. Anthropol. 57, 631–635.

MacLarnon, A.M., 1993. The vertebral canal. In: Walker, A., Leakey, R.E.F. (Eds.), The Nariokotome *Homo erectus* Skeleton. Springer-Verlag, Berlin, pp. 359–390.

MacLarnon, A.M., Hewitt, G.P., 1999. The evolution of human speech: The role of enhanced breathing control. Am. J. Phys. Anthropol. 109, 341–363.

MacLarnon, A.M., Hewitt, G.P., 2004. Increased breathing control: another factor in the evolution of human language. Evol. Anthropol. 13, 181–197.

Marino, E.A., 1995. Sex estimation using the first cervical vertebra. Am. J. Phys. Anthropol. 97, 127–133.

Martin, H., 1923. L'Homme fossile de la Quina. Librairie Octave Doin, Paris.

Martínez, I., 1995. La base del cráneo y el hueso temporal en la evolución de los homínidos, con especial referencia a los fósiles de la Sierra de Atapuerca (Burgos). Ph.D. Dissertation, Universidad Complutense de Madrid.

Martínez, I., Arsuaga, J.L., 1997. The temporal bones from Sima de los Huesos middle Pleistocene site (Sierra de Atapuerca, Spain). A phylogenetic approach. J. Hum. Evol. 33, 283–318.

Martínez, I., Rosa, M., Arsuaga, J.L., Jarabo, P., Quam, R., Lorenzo, C., Gracia, A., Carretero, J.M., Bermúdez de Castro, J.M., Carbonell, E., 2004. Auditory capacities in middle Pleistocene humans from the Sierra de Atapuerca in Spain. Proc. Natl. Acad. Sci. U.S.A. 101, 9976–9981.

McCown, T.D., Keith, A., 1939. The Stone Age of Mount Carmel. The Fossil Human Remains from the Levalloiso-Mousterian. Clarendon Press, Oxford.

Meyer, M.R., 2005. Functional biology of the *Homo erectus* axial skeleton from Dmanisi, Georgia. Ph.D. Dissertation, University of Pennsylvania.

Meyer, M.R., Lordkipanitze, D., Vekua, 2006. Evidence for the anatomical capacity for spoken language in *Homo erectus*. Am. J. Phys. Anthropol. 42 (Suppl.), 130.

Ogilvie, M.D., Hilton, C.E., Ogilvie, C.D., 1998. Lumbar anomalies in the Shanidar 3 Neandertal. J. Hum. Evol. 35, 597–610.

Pap, I., Tillier, A.-M., Arensburg, B., Chech, M., 1996. The Subalyuk Neanderthal remains (Hungary): a re-examination. Annales Historico-Naturales Musei Nationalis Hungarici 88, 233–270.

Pérez, P.-J., 2003. Recopilación de diagnósticos paleopatológicos en fósiles humanos, con casos relativos a homínidos de Atapuerca. In: Isidro, A., Malgosa, A. (Eds.), Paleopatología. La Enfermedad no Escrita. Masson, Barcelona.

Piveteau, J., 1966. La Grotte de Regourdou (Dordogne). Paléontologie humaine. Ann. Paléontol. 52, 163–194.

Radovcic, J., Smith, F.H., Trinkaus, E., Wolpoff, M.H., 1988. The Krapina Hominids. An Illustrated Catalog of Skeletal Collection. Mladost, Croatian Natural History Museum, Zagreb.

Rak, Y., Arensburg, B., 1987. Kebara 2 Neanderthal pelvis: first look at a complete inlet. Am. J. Phys. Anthropol. 73, 227–231.

Rak, Y., Kimbel, W.H., Hovers, E., 1994. A Neandertal infant from Amud Cave, Israel. J. Hum. Evol. 26, 313–324.

Rak, Y., Kimbel, W.H., Hovers, E., 1996. On Neandertal autapomorphies discernible in Neandertal infants: a response to Creed-Miles *et al.* J. Hum. Evol. 30, 155–158.

Ramírez Rozzi, F.V., Bermúdez de Castro, J.M., 2004. Surprisingly rapid growth in Neanderthals. Nature 428, 936–939.

Rosas, A., Bastir, M., Martínez-Maza, C., Bermudez de Castro, J.M., 2002. Sexual dimorphism in the Atapuerca-SH hominids: the evidence from the mandibles. J. Hum. Evol. 42, 451–474.

Scheuer, L., Black, S., 2000. Developmental Juvenile Osteology. Academic Press, San Diego.

Schiess, R., Haeusler, M., Langenegger, E., 2006. How pathological is the Nariokotome boy KNM-WT 15000 (*Homo erectus*)? Am. J. Phys. Anthropol. 42 (Suppl.), 159.

Sládek, V., Trinkaus, E., Hillson, S.W., Holliday, T.W., 2000. The People of the Pavlovian. Skeletal Catalogue of the Gravettian Fossil Hominids from Dolní Věstonice and Pavlov. Academy of Sciences of the Czech Republic, Institute of Archaeology in Brno, Brno.

Smith, B.H., 1991. Dental development and the evolution of life history in Hominidae. Am. J. Phys. Anthropol. 86, 157–174.

Stewart, T.D., 1962. Neanderthal cervical vertebrae with special attention to the Shanidar Neanderthals from Iraq. Bibl. Primatol. 1, 130–154.

Trinkaus, E., 1983. The Shanidar Neandertals. Academic Press, New York.

Trinkaus, E., 1985. Pathology and the posture of the La Chapelle-aux-Saints Neandertal. Am. J. Phys. Anthropol. 67, 19–41.

Tubbs, R.S., Wellons, J.C., Banks, J., Blount, J.P., Oakes, W.J., 2002. Quantitative anatomy of the transverse ligament tubercles. J. Neurosurg. Spine 97, 343–345.

Vandermeersch, B., 1981. Leshommesfossiles de Qafzeh (Israël). CNRS, Paris.

Vandermeersch, B., Trinkaus, E., 1995. The postcranial remains of the Régourdou 1 Neandertal: the shoulder and arm remains. J. Hum. Evol. 28, 439–476.

Walker, A., Zimmerman, M.R., Leakey, R.E.F., 1982. A possible case of hypervitaminosis A in *Homo erectus*. Nature 296, 248–250.

Wescott, D.J., 2000. Sex variation in the second cervical vertebra. J. Forensic Sci. 45, 462–466.

Winters, J.M., Peles, J.D., 1990. Neck muscle activity and 3-D head kinematics during quasi-static and dynamic tracking movements. In: Winters, J.M., Woo, S.L.-Y. (Eds.), Multiple Muscle Systems. Biomechanics and Movement Organization. Springer-Verlag, New York, pp. 461–480.